



Published in final edited form as:

*Chem Soc Rev.* 2017 May 09; 46(9): 2479–2496. doi:10.1039/c7cs00095b.

## The Aqueous Supramolecular Chemistry of Cucurbiturils, Pillar[*n*]arenes and Deep-Cavity Cavitands

James Murray<sup>a</sup>, Kimoon Kim<sup>a</sup>, Tomoki Ogoshi<sup>b,c</sup>, Wei Yao, and Bruce C. Gibb<sup>d</sup>

<sup>a</sup>Center for Self-assembly and Complexity (CSC), Institute for Basic Science (IBS), Pohang 37673, Republic of Korea

<sup>b</sup>Graduate School of Natural Science and Technology, Kanazawa University, Kakuma-machi, Kanazawa, 920-1192, Japan

<sup>c</sup>JST, PRESTO, 4-1-8 Honcho, Kawaguchi, Saitama, 332-0012, Japan

<sup>d</sup>Department of Chemistry, Tulane University, New Orleans, Louisiana 70118

### Abstract

This tutorial review summarizes the continuing exploration of three prominent water-soluble hosts: cucurbiturils, pillar[*n*]arenes and deep-cavity cavitands. As we describe, these hosts are revealing how orchestrating the Hydrophobic Effect can lead to a broad range of properties and applications, from: nano-reactors, supramolecular polymers, stimuli-responsive biointerfaces, switches, and novel purification devices. We also describe how their study is also revealing more details about the properties of water and aqueous solutions.

### Introduction

Aqueous supramolecular chemistry is dominated by two interrelated topics: the Hydrophobic Effect and the Hofmeister Effect. The first of these pertains to how non-polar molecules dissolve (or do not dissolve) in water,<sup>1</sup> whilst the second pertains to how salts modulate the properties of water and aqueous solutions; one prominent example of which is how salts modulate the Hydrophobic Effect.<sup>2</sup> Though we do not have a full understanding of these phenomena, especially at the molecular level,<sup>3</sup> we do know that the Hydrophobic Effect is dependent on both size<sup>4</sup> and shape<sup>5</sup> of a solute. It also seems to be the case that contrary to previous thoughts, the Hofmeister Effect does not control the Hydrophobic Effect by changing the properties of water itself. Rather, recent evidence suggests that instead of indirectly influencing a solute, the cation and anion of a salt directly interact with a solute. There is still much to learn about these phenomena, but in the mean time supramolecular chemists, having recently identified some fascinating new kinds of water-soluble hosts, have forged ahead with attempting to learn how the Hydrophobic Effect can be harnessed. This tutorial review takes three prominent hosts, cucurbiturils, pillar[*n*]arenes, and deep-cavity cavitands, and summarizes how their distinctive structures engender

properties intimately tied to their form. We hope that in doing so we inspire others to delve into the murky waters of aqueous supramolecular chemistry.

## Cucurbit[*n*]urils

### Preamble

Cucurbit[*n*]urils (CB[*n*] = 5–8, 10, 13–15) are a family of macrocyclic molecules with remarkable aqueous host-guest chemistry. They are composed of *n* glycoluril units bridged by *2n* methylene units to form a macrocycle with a hydrophobic cavity that is accessible by two identical portals (Fig. 1). CB[6] was the first of these to be synthesized in 1905 by Berhend, but the structure was not known until it was solved by Mock in the 1980s. CB[6] was studied as a molecular container with interesting properties, including the rate acceleration of regiospecific reactions. The CB[*n*] family<sup>6</sup> was introduced by Kim<sup>7</sup> and Day<sup>8</sup> in the early 2000s. By heating glycoluril and formaldehyde under acidic conditions at high temperature (110 °C) the thermodynamic product, CB[6], is formed almost exclusively; however, at lower temperatures (75–100 °C) the kinetic products of the reaction (mainly CB[5], CB[7], and CB[8]) along with CB[6] can be produced and isolated, along with a small amount of the larger homologues. In 2016, two more members of the CB family were isolated, CB[13] and CB[15].<sup>9</sup> Like CB[14], they adopt a twisted structure. Much of the early work on CB[*n*] including Mock's structural characterisation of CB[6] and early investigations into the host-guest chemistry in the 1980s, the characterisation of the properties of CB[*n*] (*n* = 5–8, 10) and the emerging host-guest chemistry of the newly discovered homologues was reviewed thoroughly by Isaacs in 2005.<sup>10</sup> The remarkably inert environment inside the cavity of CB[*n*] is more like the gas phase than any other form of matter because there is very little electron density in the cavity itself; there are no functional groups or lone pairs of electrons pointing inward. Consequently, CB[*n*] show a preference for guests that are hydrophobic and have good size complementarity with the cavity. Each portal is made from *n* ureido carbonyls; the proximity of these carbonyls leads to a ring that is very electronegative (Fig. 2). The effect of the electrostatic potential is manifested in the host-guest chemistry: all CB[*n*] show a distinct preference to interact with cationic species over neutral species and even more so over anionic species. The portal diameter is generally smaller than that of the cavity, which results in host-guest complexes with low dissociation rates. Generally, CB[*n*] prefer amphiphilic guests that combine a cationic group with a hydrophobic core. The aqueous solubility of the CB[*n*] family varies by member. CB[5] and CB[7] show moderate water solubility (20–30 mM) whereas CB[6] and CB[8] are much less soluble in water. Their solubility increases in acidic solutions, since the carbonyl portals interact with hydronium ions facilitating the dissolution. Under neutral conditions, the addition of alkali metal salts is also an efficient solubilizing method. Furthermore, the solubility of the CB[*n*] tends to increase upon incorporating a guest molecule; especially a positively charged one. Despite their relatively low solubility, there are therefore several ways that the host-guest chemistry of CB[*n*] can be translated into aqueous chemistry applications. The combination of these properties has allowed the realisation of many aqueous chemistry applications. CB[*n*] applications include acting as reaction containers, as a tool to functionalize planar and particulate surfaces, and in sensing. There have been several reviews published recently which outline these applications as well as the

fundamental studies on CB[*n*] host-guest chemistry.<sup>11–14</sup> In this review, two unique features of CB chemistry are highlighted. First, the ability of CB[8] to form ternary complexes and how this can be utilized to build supramolecular assemblies and functionalize aqueous interfaces. Second, the remarkably high-affinity binding of CB[7] towards ferrocene, adamantane and other ammonium-derived guests in water.

### The Curious Case of CB[8]

The standout feature of CB[8] is its ability to form ternary complexes with either 1:2 (host: guest) or 1:1:1 (host: guest1: guest2) stoichiometry with a variety of guest molecules. Among these, charge-transfer (CT) complexes, where one guest is a  $\pi$ -donor and the other is a  $\pi$ -acceptor, form particularly stable ternary complexes. CT complexes can form supramolecular assemblies, such as rotaxanes and catenanes, spontaneously; they can be further stabilized when encapsulated in CB[8]. The first example reported by Kim and co-workers<sup>15</sup> consisted of methyl viologen ( $MV^{2+}$ ,  $\pi$ -acceptor) and 2,6-hydroxynaphthalene (HN,  $\pi$ -donor), which forms a stable charge transfer complex inside CB[8] spontaneously. The host markedly enhances the CT interaction to give a stable ternary complex. Complexes of this type form spontaneously when the components are mixed in a 1:1:1 ratio. The complexes also form in a step-wise manner; the electron-deficient guest binds first to CB[8] and the electron rich component is incorporated second (a process that is often very exothermic). The electron-rich guest does not bind to CB[8] in the absence of an electron poor guest. This well-defined donor-acceptor behaviour provides a unique opportunity to construct, stable supramolecular assemblies in water and at aqueous interfaces. The donor-acceptor moieties can be incorporated into the same molecule (D-A), which can then interact with CB[8] to give a range of assemblies that varies in complexity. For example, a D-A molecule can form a looped 1:1 complex or a linear 2:2 stacked complex, which can also be extended into a supramolecular polymer or into a cyclic ‘molecular necklace’. The earlier work on the construction of supramolecular assemblies based on the host-stabilised CT complex formation was reviewed by Kim.<sup>16</sup> Scherman has used CB[8] extensively in the preparation of supramolecular block copolymers, which can also be extended into 3D-networks; this important contribution to the field is discussed in Scherman’s recent review and the references therein.<sup>12</sup> More recently, Scherman has integrated microfluidics and host-guest chemistry to construct CB[8]-based microcapsules inside droplets.<sup>17</sup> The use of CB[8] to construct these microcapsules bestows stimuli responsiveness to the formed materials and may have applications as responsive cargo delivery vehicles. Another of CB[8]’s interesting features is that it has intrinsic affinity with specific peptide sequences that allows the formation of peptide-based charge-transfer complexes. Aromatic amino acids can act as electron-poor components of a charge transfer complex; therefore, they can form host-stabilized complexes with CB[8] and  $MV^{2+}$ . Urbach and co-workers have been the pioneers in this area; they found that tripeptides containing one tryptophan and two glycine residues (WGG, GWG, GGW) form CT-complexes with CB[8] and  $MV^{2+}$ , and that the closer the aromatic residue is to the *N*-terminus the stronger the interaction. Scherman and co-workers have exploited this by using CB[8] and  $MV^{2+}$  as an electrochemically responsive system to capture *N*-terminal-tryptophan-containing peptides. *N*-terminal tryptophan is an electron rich species which forms a CB[8]-stabilized CT-complexes with  $MV^{2+}$ . Thiol labelled  $MV^{2+}$  was immobilized onto a gold surface; these viologens were then threaded

with CB[8]. The surface was then primed to selectively capture N-terminal-tryptophan-containing peptides. From a mixture of peptides, only N-terminal tryptophan peptides were immobilized. Furthermore, the  $MV^{2+}$  can be reduced to  $MV^{+•}$  causing the complex to dissociate and release the peptides. Not only can a CB[8]- $MV^{2+}$  surface be used to capture simple biomolecules it can also be used to control cell adhesion to a surface. Jonkheijm and Huskens have used a similar CB[8]- $MV^{2+}$  surface; however, they employed a simple peptide with an N-terminal tryptophan (a  $\pi$ -donor) possessing an RGD group (a peptide sequence that is known to adhere to cells) as the third component in the ternary complex. When the ternary complex was formed the RGD group was available for binding, which allowed cells to adhere to the surface. When the  $MV^{2+}$  was electro-chemically reduced, the complex dissociated and the tryptophan-containing RGD peptide was released, causing the cells to detach from the surface. The peptide array can be regenerated by re-oxidising  $MV^{+•}$  back to  $MV^{2+}$ . Scherman and coworkers have extended this principle to prepare a surface with two orthogonal switching mechanisms (Fig. 3). As well as using redox chemistry, they also use a light responsive CB[8] guest, azobenzene. The surface was functionalized with azobenzene and the methyl viologen and CB[8] were added from solution. This allowed the preparation of a tristable system that may be useful for preparing responsive surfaces at biointerfaces or for memory applications. The reader is directed to a recent review (and the references therein) by Zhang and Scherman on the use of supramolecular chemistry to functionalize aqueous interfaces for the original work.<sup>18</sup>

### Ultra-High Affinity CB-guest Pairs

CB[*n*]s shows very high affinities for specific guests and discriminates based on charge and shape. For example, CB[*n*] affinity has been reported to be as high as  $10^{17} M^{-1}$ , and they show selectivity for cationic species, moderate affinity for neutral guests and little affinity for anionic species. The charge selectivity can be easily rationalized by considering the highly polarized ureidyl portal that can make ion-dipole interactions with cationic guests. While most macrocycles exhibit an enthalpy dominated hydrophobic effect, it does not usually manifest as high binding affinity. In the case of CB[*n*] (CB[7], in particular) the enthalpic contributions and resultant binding affinities are exceptionally high because of the unfavourable interactions water molecules experience in the CB[*n*] cavity. In this section, we shall discuss the design and binding affinities of high-affinity guests for CB[7] and describe the thermodynamic basis of this high affinity. Finally, we will showcase some of the notable applications of these high-affinity host-guest pairs. The first high guest affinities for CB[7] were measured in 2005 by Isaacs<sup>19</sup> (NMR) and in a parallel study by the groups of Kim, Inoue, and Kaifer (ITC).<sup>20</sup> The latter study showed that the neutral ferrocene derivative **F1** (Fig. 4) binds CB[7] with  $K_a = 10^9 M^{-1}$ , since it is hydrophobic and has very good size complementarity with CB[7], thereby filling the cavity effectively. Higher affinity guests can be achieved by addition of a cationic group, di(or tri)alkylmethylammonium, onto the ferrocene core (Fig. 4). The cationic ferrocene derivatives **F2** and **F3** have affinities of  $K_a = 10^{12} M^{-1}$ . At the time these were the highest affinity, monovalent binding pairs known. The high affinity of neutral ferrocene and 1000-fold affinity increase upon the addition of the cationic group suggests that the ferrocene is well-positioned in the CB[7] cavity and the cationic group is in an ideal position to make an ion-dipole interaction with the portal. In 2007, the groups of Inoue, Kim, Isaacs, Kaifer, and Gilson<sup>21</sup> wondered whether a higher

affinity guest could be realized by the addition of a second cationic group. Indeed, this is the case, *bis*-trimethylammonium ferrocene (**F4**) has a binding affinity for CB[7] of  $10^{15} \text{ M}^{-1}$ , measured by ITC. This was a significant milestone because it was the first synthetic host-guest pair to surpass that of biotin-(strept)avidin (Bt-SA), which is the benchmark high-affinity binding pair in nature. The X-ray structure of this complex shows that it is symmetrical and both trimethylammoniums protrude from the cavity, the ferrocene unit is slightly tilted to make ion-dipole interactions with the portal. The diamantane is a symmetrical aminoadamantane with a cationic group (trimethyl-ammonium) on both sides, both cationic groups are ideally placed to make the ion-dipole interactions with both portals. Furthermore, the diamantane group effectively fills the cavity, these two factors should make for an exceptionally high-affinity guest. The affinity measured by NMR was so high to have an attomolar ( $10^{-18} \text{ M}$ ) dissociation constant. This is currently the highest synthetic binding pair known. The binding constants for these guests are shown in Figure 4. There are two common features that these guests share: First, the hydrophobic cores are rigid and complement the CB[7] cavity; second, the ammonium groups of the guest are ideally positioned to make ion-dipole interactions with one or both portals. Generally, complexation events exhibit enthalpy-entropy compensation, whereby a favourable enthalpic contribution caused by the newly introduced functional group is offset by an unfavourable entropic penalty. One of the many potential bases for this phenomenon is that the newly introduced non-covalent interaction that increases the enthalpy of association also leads to an associated increase in configurational restriction of the guest.<sup>23</sup> Cyclodextrins exhibit this effect very well as shown in the plot (Fig. 5), but when high-affinity cucurbituril guests are added to this plot, it is clear that they do not follow the same trend. When the binding affinities are deconstructed into their enthalpic and entropic contributions the reasons for the high binding affinities becomes clearer (Fig. 4). When the neutral hydroxymethyl of the neutral ferrocene **F1** is replaced with methylammonium derivatives the enthalpy is unperturbed ( $\Delta H^{\circ} = -21 \text{ kcal mol}^{-1}$ ), but the entropy penalty decreases ( $3.8\text{--}4.3 \text{ kcal mol}^{-1}$ ) and this is responsible for the 1000-fold enhancement in binding affinity; the pattern repeats on the addition of a second methylammonium group. There are several remarkable things here: First, **F1** binds to CB[*n*] mainly by hydrophobic interactions and the enthalpy contribution to this interaction is remarkably large compared to other host-guest systems. Secondly, there is no additional enthalpy gain by addition of an ammonium to the guest (F2–F4), which makes an ion-dipole interaction. Instead, the 1000-fold increase in binding affinity per cation is driven, entropically, by the desolvation of the portals and the guest's cation(s).

The enthalpy-driven hydrophobic effect exemplified by cucurbiturils has been investigated in detail by the group of Nau and has been summarized recently,<sup>24</sup> so it will only be discussed briefly here. The structural features of CB[*n*] maximize this enthalpy-dominated hydrophobic effect because the cavity is very apolar and the rigid structure means no reconfiguration is possible to alleviate the energetic frustration of the cavity water molecules. The extreme enthalpically-driven hydrophobic effect is most evident in the case of the neutral ferrocene derivative **F1**, which has a binding of  $10^9 \text{ M}^{-1}$ , and  $\Delta H^{\circ} -21 \text{ kcal mol}^{-1}$  which is remarkably high for a hydrophobic interaction. For comparison,  $\beta$ -cyclodextrin (which has a similar size cavity to CB[7]) binding affinities rarely exceed  $10^6 \text{ M}^{-1}$ . Simulations have suggested that the water molecules in the CB[7] cavity have a lower

hydrogen bond count than those in the bulk solution. Therefore, the cavity may possess a drying transition and host-guest complexation would therefore not have to compete with pocket desolvation. This enthalpy-dominated hydrophobic effect is maximal for CB[7], since CB[6] has a smaller cavity with less potential for dewetting, and CB[8] is larger and the simulated water molecules are closer to that of the bulk solution; experimentally, it has been shown the  $\Delta H$  value is lower for CB[6] and CB[8] than it is for CB[7]. Another case where desolvation of the cavity is enthalpically dominated is when CB[8] forms a ternary complex. Upon complexation of the first guest, the remaining cavity volume is much smaller and possess a similar dewetting potential to CB[7]. As expected, the addition of the second guest is strongly exothermic, especially when the guest completely desolvates the cavity such as the CT-complexes described above. Nau and co-workers have shown the lower hydrogen bond count of the cavity water molecules is important in these systems by demonstrating a solvent and solvent isotope effect on binding affinity. In acetonitrile, the binding affinity is 1000-fold less, and the second guest binding is more exothermic in water than in deuterium oxide because the hydrogen bonds are stronger than deuterium bonds. Overall, multiple studies have demonstrated the importance of the enthalpy-dominated Hydrophobic Effect in the high-affinity binding of cucurbiturils. The reader is directed to the reviews by Nau<sup>24</sup> and Kim<sup>11</sup> and the references therein for the original studies. Furthermore, the ion-dipole interaction seems to be almost entirely *entropy*-dominated caused by the desolvation of the cation and portal upon guest binding, which is shown by the deconstructed thermodynamic data with various ferrocene derivatives.

Since the high-affinity CB[7] host-guest pairs now approach - and even surpass - the biotin Streptavidin (Bt-SA) interaction, this raises the question: can these pairs be applied as widely as the natural pair? Soon after the high-affinity host-guest pairs were discovered they were used as replacements for Bt-SA, and in some cases, may eventually supplant the natural binding pair. The advantages of the CB[7] system include that it is resistant to enzymatic degradation and the binding may be modulated or reversed by a competitor guest or by changing the redox state of the guest molecule. The applications of the CB[7] system include biomolecule immobilization, protein enrichment, adhesive materials, high-affinity FRET-pairs, therapeutic activation of nanoparticles, and regulation of biological catalysis. These applications have been reviewed recently, along with methods to functionalize CB[7] to better harness its properties in materials applications. We will highlight a few of these applications here; the reader is directed to the review by Kim and the references therein for the original works.<sup>11</sup> The first example of such an application was the immobilization of a protein onto a self-assembled monolayer (SAM). An allyl-functionalized CB[7] was attached to an allyl-terminated SAM by employing a metathesis reaction. This CB[7] functionalized surface was able to anchor ferrocene-labelled (“ferrocenylated”) glucose oxidase (Fc-GOx) to the surface. Since GOx is redox active, this surface was used as a biosensing platform for glucose. In a similar vein, Kim and co-workers prepared a CB[7]-bead analogous to a streptavidin (SA) functionalized bead. In the life sciences, SA-beads are often used to capture biotinylated proteins to enrich a protein of interest. However, SA-beads can also capture endogenously biotinylated proteins, and release of the biotinylated proteins from the beads, or post-enrichment, requires very harsh conditions. The CB[7] bead is able to selectively capture ferrocenylated proteins (in this case membrane proteins) and after



enrichment, the ferrocenylated proteins are released simply by incubation with a higher affinity guest, **F4** (Fig 6). Another interesting application is the development of an underwater adhesion system. Velco<sup>®</sup> works by fastening hooks into loops, and Kim and co-workers wondered if this kind of attachment could be replicated at the molecular level using a CB[7]-functionalized surface (the loop) and a complimentary cationic ferrocene-functionalized surface (the hook). When the surfaces are wet, they adhere to each other; these can either be separated by mechanical force or by oxidation of the ferrocene with hypochlorite solution. This work represents the transformation of a molecular recognition event into a macroscopic property (Fig. 7). CB[7] can also be functionalized for solution-based applications, for example, Kim and co-workers have prepared a Cy3-functionalized CB[7] and used this to form a high-affinity FRET-pair with a Cy5-functionized adamantane. This pair was used in a vesicle mixing assay, whereby each component was reconstituted into an individual vesicle, and when these vesicles were mixed, a FRET-signal was observed. The most interesting finding from this work was direct observation of flickering-fusion events caused by transient opening and closing of the pore formed between the vesicles. This work emphasizes the power of using a simple synthetic system for examining a complex process.

Moving to therapeutic applications Rotello and Isaacs have used a CB[7]-based system to pacify and then activate cytotoxic nanoparticles in response to a chemical stimulus (Fig 8). The cytotoxic nanoparticles were prepared by functionalizing a gold-nanoparticle terminated with diamino-hexane. When these nanoparticles were treated with CB[7], the CB[7] moiety caps the amines and renders the particle non-cytotoxic, by virtue of it becoming trapped in the endosome after uptake. Upon addition of a high-affinity guest, **A2**, the CB[7] cap is removed since CB[7] forms a more favourable complex with **A2**. This triggers endosomal escape of the nanoparticles into the cytosol, thereby activating the cytotoxicity. This work is significant in that it shows that CB[7] system is robust and selective enough to be activated in *in vivo* conditions and may have important applications in drug delivery. Isaacs and co-workers have demonstrated control of biological catalysis using CB[7]. By preparing a bifunctional molecule that is able to bind both CB[7] and bovine carbonic anhydrase (BCA), a supramolecular switch was prepared. The molecule binds to BCA, thereby inhibiting its catalytic activity, but upon addition of CB[7] the extra steric bulk causes the inhibitor to dissociate and reactivates the catalytic activity. The process can be reversed by addition of trimethylsilyl-methylammonium, a moderate-to-high affinity guest for CB[7] ( $K_a \sim 10^9 \text{ M}^{-1}$ ) that causes the release of the two-faced molecule, which in turn re-inhibits the BCA.

The signature high-affinity binding of the CB[*n*] family is in large part a result of CB[*n*]'s poor interactions with water. The narrower portal of CBs relative to cyclodextrins may make their pockets more inhospitable to water because each water molecule encapsulated must accept a lower H-bond count than it would in the bulk solution; the filling of the cavity with a hydrophobic guest is therefore very exothermic. The polar portals are well solvated in water and desolvation of the portal (and a cationic guest) by making an ion-dipole interaction between host and guest is very entropically favourable, leading to a 1000-fold increase in binding in some cases.

These unusual thermodynamic effects are particularly apparent in CB[7], but similar high-affinity binding is also apparent in CB[8] systems. The addition of a second guest in the formation of a CB[8] stabilized-CT-complex is also subject to an enthalpy-dominated Hydrophobic Effect. Not only does CB[8] form stable assemblies but they can also be switchable, for example by redox chemistry, and this has been exploited as a tool to prepare stimuli-responsive (bio)interfaces. The exceptional stability, biocompatibility, and ease of handling means that the CB[7] system may compliment –or even supplant– Bt-SA for some applications. Recent progress in the field suggests that high-affinity binding pairs are making the transition from basic research into important applications.

## Pillar[*n*]arenes

### Preamble

Pillar[*n*]arenes are a family of pillar-shaped or cylindrical cyclic hosts possessing aromatic walls (Fig. 9).<sup>25–30</sup>

Similar to the calix[*n*]arenes, the repeating units of pillar[*n*]arenes are phenolic moieties; however, in pillar[*n*]arenes, the repeating units are connected by methylene bridges at their 2- and 5-positions (i.e., in the para-positions), whereas the repeating units in calix[*n*]arenes are linked by methylene bridges at their 2- and 6-positions (meta-positions). It is this difference that leads to pillar[*n*]arenes possessing pockets that are open at both ends, i.e., they are of cylindrical form in contrast to the conical calixarenes. Inspired by the highly symmetrical pillars that constitute the Parthenon in Athens (Fig 9b), in 2008 Ogoshi named these new macrocyclic hosts “pillar[*n*]arenes”.<sup>25</sup> The pillar-shaped structure has a large influence on the physical properties of pillar[*n*]arenes. One important feature is their host-guest properties; pillar[*n*]arene units are constructed from electron-rich (donating) 1,4-dialkoxy-benzenes, which gives the cavity an affinity for electron-deficient guests. Furthermore, the cylindrical structure very efficiently enhances the  $\pi$ -electron density in the cavity (Fig. 9c). In contrast, the  $\pi$ -electron density enhancement is not efficient in the cavity of calix[*n*]arenes because the calix-shaped structures are not the ideal platform for this enhancement. The electron-rich cavity of pillar[*n*]arenes means that they prefer to bind molecules with cationic moieties, such as pyridinium, viologen and ammonium moieties. However, Li and co-workers discovered very strong complexation between simple alkylated pillar[5]arenes and neutral linear molecules with electron-withdrawing groups at the termini. The association constants for these systems were in the vicinity of  $10^4 \text{ M}^{-1}$ , which indicates a surprisingly efficient host-guest interaction, particularly in organic media. Among various hosts, the cucurbit[*n*]urils form some of the strongest complexes, but these complexes are formed not in organic, but in aqueous media.

Pillar[*n*]arenes consist of hydrophobic cores of aromatic and methylene bridges and have substituents on both rims. An important advantage of pillar[*n*]arene chemistry is that the core pillar[*n*]arene macrocyclic structure is easy to construct. Numerous synthetic pathways have been investigated for the preparation of pillar[*n*]arenes, and a simple and easy pathway is the reaction of 1,4-dialkoxybenzene with paraformaldehyde and an appropriate acid. The solvents used for the reaction play a major role in determining the number of repeating units (Fig. 9a). Cyclic pentamers pillar[5]arenes are prepared in high yields when 1,2-



dichloroethane is used as the solvent. 1,2-Dichloroethane is a linear molecule with electron-withdrawing chlorine moieties at both ends, and thus acts as a template solvent in the formation of pillar[5]arenes. In contrast, mixtures of larger pillar[*n*]arene homologues and linear oligomers are obtained when chloroform is used as the solvent. Unlike 1,2-dichloroethane, chloroform does not act as a template for pillar[5]arenes because it has three chlorine moieties, which does not fit to this particular pillar[*n*]arene homologues. The bulky solvent chlorocyclohexane is one of several good template solvents for the synthesis of pillar[6]arenes because the cavity size of pillar[6]arenes (ca. 6.7 Å) is larger than that of pillar[5]arenes (ca. 4.7 Å), and fits to the bulky solvent chlorocyclohexane. An important advantage of pillar[*n*]arenes compared with other host molecules is their versatile functionality.<sup>28</sup> The alkoxy substituents on both rims of pillar[*n*]arenes can be readily converted to reactive moieties such as phenol, bromide, azide and alkyne moieties (Fig. 9a). Substrates with reactive phenolic moieties can be synthesised by deprotection of the alkoxy substituents of pre-formed pillar[*n*]arenes. Pillar[*n*]arenes bearing bromide and alkyne moieties are accessible by cyclisation of the corresponding 1,4-dialkoxybenzenes with two bromide and two alkyne moieties. Pillar[*n*]arenes with azido moieties can be readily prepared by reaction of pre-formed bromide derivatives and sodium azide. These three types of pillar[*n*]arenes are useful key compounds for the preparation of further functionalised pillar[*n*]arenes. Etherification is a straightforward pathway to functionalise pillar[*n*]arenes from phenol derivatives. Cationisation and etherification can be used to functionalise bromide-substituted pillar[*n*]arenes. Copper(I)-catalysed alkyne-azide cyclisation (CuAAC) reactions between alkyne-bearing pillar[*n*]arenes and monoazides or azido-functionalised pillar[*n*]arenes and monoalkynes are facile and useful methods for producing various functionalised pillar[*n*]arenes. The substituents on both rims also determine the physical properties of the pillar[*n*]arenes, such as their solubility, and conformational and host-guest properties, because the pillar[*n*]arene cores are surrounded by these functional substituents. It is therefore possible to design various highly functionalised pillar[*n*]arenes based on this versatile functionality.

### Synthesis and Properties of Water-Soluble Pillar[*n*]arenes

Pillar[*n*]arenes with hydrophobic chains, such as those with simple alkyl and phenolic substituents, are not water-soluble. Therefore, host-guest complexation using these pillar[*n*]arenes is mainly investigated in organic solvents. However, per-functionalisation is a convenient way of altering the solubility properties of pillar[*n*]arenes because their solubility depends on the substituents that surround the pillar[*n*]arene core. Introducing hydrophilic moieties, such as cationic or anionic groups onto both rims of pillar[*n*]arenes can afford water-soluble pillar[*n*]arenes (Fig. 10). Ogoshi and coworkers first synthesised a water-soluble pillar[5]arene by modification with carboxylate anions on the pillar[5]arene rims (Fig. 10a).<sup>31</sup> First, ethoxycarbonylmethoxy-substituted pillar[5]arene was synthesised by etherification. Subsequent hydrolysis of the ethoxy moieties under basic conditions afforded pillar[5]arene **H1**, containing 10 carboxylate centers. The presence of 10 negative charges makes it possible for this pillar[5]arene to act as a cation receptor in water. For example, when **H1** was mixed with cationic viologen salt **G1**, namely paraquat, a 1:1 host-guest complex was formed. The association constant of the complex determined by fluorescence measurements was  $(8.2 \pm 1.7) \times 10^4 \text{ M}^{-1}$ , which is almost 70 times higher than that of the

complex formed between paraquat and a pillar[5]arene containing 10 phenolic moieties in methanol; in aqueous media, the Hydrophobic Effect, electrostatic interactions between cationic paraquat **G1** and the carboxylate anions on the rims of **H1**, and the charge-transfer interaction between host and guest all combine to promote binding. Li, Jia, and co-workers investigated the complexation behaviour of 20 amino acids with **H1**.<sup>32</sup> **H1** showed highly selective binding ( $K = \text{ca. } 10^3 \text{ M}^{-1}$ ) towards amino acids such as L-arginine **G2**, L-lysine **G3** and L-histidine **G4** compared with that towards other  $\alpha$ -amino acids ( $K = \text{ca. } 20 \text{ M}^{-1}$ ). The basic structure of amino acids contains one amino group; however, L-lysine, L-arginine, and L-histidine have additional amino groups on their side chains. Thus, the electrostatic interactions between the negative carboxylate groups on both rims of the pillar[5]arene and the multiple cationic ammonium groups in these amino acids work cooperatively to selectively bind these three amino acids.

Huang and co-workers synthesised a water-soluble cyclic hexamer, pillar[6]arene **H2**, containing 12 carboxylates, using the same approach used to synthesise host **H1**.<sup>33</sup> Water-soluble pillar[6]arene **H2** formed highly stable 1:1 host-guest complexes with paraquat **G1** [ $K = (1.02 \pm 0.10) \times 10^8 \text{ M}^{-1}$ ]. The binding constant of this complex is almost 1300 times higher than the corresponding  $K$  value for the complexation between the analogous water-soluble pillar[5]arene (**H1**) and **G1**. The high binding affinity results from the size-matching between water-soluble pillar[6]arene **H2** and paraquat **G1**; the width of the 4,4'-bipyridinium groups is 6.3 Å, which does not fit into the cavity of pillar[5]arenes (ca. 4.7 Å) without deforming the host but does fit into that of pillar[6]arenes (ca. 6.7 Å). The same group also synthesised water-soluble pillar[ $n$ ]arenes with different cavity sizes [ $n = 7$  (**H3**), 9 (**H4**) and 10 (**H5**)], and investigated their host-guest ability towards paraquat **G1**. Water-soluble pillar[7]arene **H3** formed the most stable host-guest complex with **G1** [ $K = (2.96 \pm 0.31) \times 10^9 \text{ M}^{-1}$ ] among the water-soluble pillar[ $n$ ]arene homologues (**H1**–**H5**). The water-soluble pillar[ $n$ ]arenes with large cavities can also form host-guest complexes with large guests such as naphthalene diimide **G5** and 1,10-phenanthroline diium **G6** cations.

Introduction of cationic moieties onto the pillar[ $n$ ]arene rim is another useful way of producing water-soluble pillar[ $n$ ]arenes.

Huang and co-workers were the first to introduce cationic moieties and synthesise a water-soluble pillar[5]arene (Fig. 10).<sup>34</sup> Cyclisation of 1,4-dialkoxybenzene containing two bromide moieties in 1,2-dichloroethane, which is a good template solvent for the synthesis of pillar[5]arenes, gave a pillar[5]arene containing 10 bromide moieties. Pillar[5]arene **H6**, containing 10 trimethyl ammonium groups on the upper and lower rims, was prepared by treatment of the brominated pillar[5]arene with excess trimethylamine. Because of the 10 ammonium cations on the pillar[5]arene rim, cationic pillar[5]arene **H6** is a good anion receptor and showed a high affinity for sodium alkyl sulfonates in water. For example, cationic pillar[5]arene **H6** formed a stable 1:1 host-guest complex with 1-octanesulfonate **G7** in water [ $K = (1.33 \pm 0.94) \times 10^4 \text{ M}^{-1}$ ].

Water-soluble pillar[ $n$ ]arenes can also be synthesised by modifying pillar[ $n$ ]arenes with non-ionic oligo(ethylene oxide) chains (**H7** and **H8** Fig. 10b). Modification of a pillar[5]arene

with long tri(ethylene oxide) chains made it fully soluble in water at 25 °C whereas a pillar[5]arene modified with shorter ethylene oxide chains was insoluble.

### Stimuli-Responsive Water-Soluble Pillar[n]arenes

Aqueous solutions containing tri(ethylene oxide)-substituted pillar[5]arene **H7** and pillar[6]arenes **H8** are homogeneous at room temperature, became opaque on heating, and then homogeneous again upon cooling. This indicates that tri(ethylene oxide)-substituted pillar[5]arene and pillar[6]arene exhibit lower critical solution temperature (LCST) behaviour,<sup>35</sup> which can be attributed to the combination of the hydrophilic tri(ethylene oxide) moieties and hydrophobic pillar[5]arene core. Heat-induced de-solvation of water molecules from the tri(ethylene oxide) chains triggers the aggregation of the hydrophobic pillar[n]arene cores. The cloud points of tri(ethylene oxide)-substituted pillar[5]arene **H7** and pillar[6]arene **H8** were 41 and 42 °C respectively; indicating that the differences between the cyclic pentamer and hexamer structures did not affect the clouding points. As with the anionic pillar[5]arenes, tri(ethylene oxide)-substituted pillar[5]arene **H7** formed a 1:1 host-guest complex with paraquat **G8** [ $K = (4.3 \pm 0.5) \times 10^3 \text{ M}^{-1}$ ]. As the amount of **G8** was increased in this system, the clouding points of pillar[5]arene **H7** increased from 42 to 60 °C (Fig. 11a). Repulsive forces between the complexed cations are one of the main reasons why this increase in the clouding point occurred. Cucurbit[7]uril **CB[7]** forms a very stable host-guest complex with paraquat **G8** in aqueous media ( $K > 10^5 \text{ M}^{-1}$ ); thus, **CB[7]** can be used as a competitive host to dissociate the **H7**⊃**G8** complex. Addition of **CB[7]** to the **H7**⊃**G8** complex induced the dissociation of the complex, and this led to a decrease in the clouding points of pillar[5]arene **H7** from 60 to 47 °C. As a result, it was possible to tune the clouding points of pillar[5]arene **H7** by addition of guest paraquat **G8** and competitive host **CB[7]**.

Azobenzene derivatives are widely used as photo-responsive compounds. Pillar[6]arenes form stable host-guest complexes with *trans*-azobenzene derivatives, but not with the *cis* isomers; the latter is ill-fitting. Consequently, the photo-responsive host-guest system composed of pillar[6]arenes and azobenzene derivatives can be used as a photo-switch. Thus tri(ethylene oxide)-substituted pillar[6]arene **H8** formed a host-guest complex with *trans*-azobenzene **G9**, containing two 1,4-diazabicyclo[2,2,2]octane (DABCO) cations in aqueous media [Fig. 11b,  $K = (4.3 \pm 0.5) \times 10^3 \text{ M}^{-1}$ ]. Complexation between azobenzene guest **G9** in the *trans*-form and pillar[6]arene **H8** induced an increase in the cloud points from 42 to 57 °C. The reason for this increase is the same as that described above for the pillar[5]arene **H7** ⊃ **G7** complex: electronic repulsion between the complexed cations prevents the aggregation of pillar[6]arenes **H8**. The cloud points of the complex decreased from 57 to 52 °C upon UV irradiation; a change in the conformation of azobenzene guest **G9** from the *trans*- to the *cis*-state was induced by UV irradiation, which triggered the dissociation of the host-guest complex. Hence the dissociation of the complex functioned as a switch to change the clouding point of the mixture. The cloud point of the mixture returned to 57 °C on visible light irradiation with the conversion of the *cis*-form of azobenzene guest **G9** back to the *trans*-form.

Pei and co-workers synthesised pillar[5]arene **H9** functionalised with 10 ferrocene moieties using the CuAAC reaction of an azido-functionalised pillar[5]arene and a ferrocene bearing one alkyne group (Fig. 11c).<sup>36</sup> This host was not soluble in aqueous media. However, oxidation of the ferrocenyl groups resulted in the formation of the ferrocenium cation derivative which formed spherical vesicles in aqueous media because the core of the pillar[5]arene and the ferrocenium cation substituents are hydrophobic and hydrophilic respectively. Reduction of the ferrocenium cations with glutathione (GSH) acted as a trigger for the release of a drug encapsulated in the vesicles. This GSH-responsive system would be an ideal drug/siRNA co-delivery system for drug release and gene transfection in cancer cells because the GSH concentration in cancer cells is typically higher than that in normal cells.

### Applications of Water-Soluble Pillar[n]arenes

Pillar[n]arenes have a cylindrical structure, and can thus be used as artificial channels for molecular transportation. Hou and co-workers reported artificial single-molecular transmembrane water channels using pillar[5]arenes bearing hydrazide moieties on their side chains (Fig. 12a, **H10** and **H11**).<sup>37</sup> The hydrazide units participated in intramolecular hydrogen bonding to produce the tubular structure. These tubular molecules acted as channels for transporting water across a liquid membrane when they were inserted into the membranes. The water transport from outside to inside the vesicles was driven by the osmotic pressure difference between the outside and inside of the vesicles. Thus, the transport of water molecules caused swelling and fusion of the vesicles. The pillar-shaped structure of pillar[n]arenes is also useful for constructing multi-layer structures using layer-by-layer (LbL) assembly. In most cases, polymer systems are used in LbL assembly because multiple interaction points, which are observed in polymer systems, are necessary for construction of thin films using this technique. LbL assembly of molecules with low molecular weights is generally difficult and comparatively rare because of the lack of multiple interaction points. However, the presence of functional groups at both rims of water-soluble cationic and anionic pillar[n]arenes allow these hosts to efficiently form multilayers using LbL assembly (Fig. 13).<sup>38</sup> First, an inorganic substrate with anionic surface charges was immersed in an aqueous solution of cationic pillar[5]arene **H6** to introduce cationic pillar[5]arenes onto the substrate by means of anion-cation interactions. Then, the substrate was immersed in an aqueous solution of anionic pillar[5]arene **H1** to introduce anionic pillar[5]arenes onto the cationic surface Wang and co-workers reported dramatic swelling of hydrogels promoted by the complexation between anionic pillar[6]arene **H2** and ferrocene groups in a hydrogel (Fig. 14).<sup>39</sup> When a hydrogel covalently functionalised with ferrocene groups was immersed in an aqueous solution of anionic pillar[6]arene **H2**, the hydrogel swelled dramatically, with an approximately 11-fold increase in weight compared with that in pure water constructed from the cationic pillar[5]arenes. Multilayer films were obtained by repeating these alternating immersion steps. This swelling was due to the formation of inclusion complexes between anionic pillar[6]arene **H2** and the ferrocene groups in the hydrogel. Because anionic pillar[6]arene **H2** contains 12 carboxylate anions, this complexation generated strong electrostatic repulsion between the polymer chains, and thus resulted in the swelling of the hydrogel.

Guest molecules can access both portals of pillar[n]arenes, and pillar[n]arenes can thus be used as the ring component in pseudo[2]rotaxane structures. Huang and co-workers have reported various supramolecular assemblies, including micelles, vesicles, and tubes, constructed from [2]pseudorotaxanes consisting of water-soluble pillar[n]arenes and amphiphilic guests.<sup>40</sup> Tubular aggregates were formed by self-assembly of amphiphilic guest **G10**, which consists of a hydrophilic pyridinium salt and hydrophobic alkyl and pyrene groups (Fig. 15). In contrast, the water-soluble pillar[6]arene **H2** and **G10** complex self-assembled to form vesicles. Typically, a high membrane curvature tends to result in nanotubular assemblies, whereas a membrane with a low curvature favours vesicular assemblies. In the absence of water-soluble pillar[6]arene **H2**, amphiphilic guest **G10** self-assembles to form a highly ordered bilayer of pyrenyl groups through  $\pi$ - $\pi$  interactions, which leads to a high curvature and the formation of tubular assemblies. In contrast, the formation of a [2]pseudorotaxane between water-soluble pillar[6]arene **H2** and amphiphilic guest **G10** disturbs the straight array of guest molecules because of the steric hindrance and electrostatic repulsion of anionic pillar[6]arene **H2**, and this then results in the formation of vesicles with a low curvature; the reversible transformation between nanotubes and vesicles was readily controlled by changing pH. The same authors also reported photo-responsive self-assembly switching between vesicles and solid nanoparticles using supramolecular amphiphiles consisting of water-soluble pillar[6]arene **H2** and an amphiphilic guest containing hydrophilic ammonium cations and hydrophobic azobenzene parts.

Nierengarten and co-workers synthesised water-soluble glycoclusters containing 10 sugar residues and a pillar[5]arene core (Fig 16a).<sup>41</sup> The synthesis of these pillar[5]arene-based glycoclusters was readily achieved by a CuAAC reaction between an alkyne-functionalised pillar[5]arene and acetylated sugar residues bearing one azide moiety. Deprotection of the acetylate ester moieties gave the water-soluble glycoclusters. The authors then investigated multivalent binding of the glycoclusters to pathogenic bacterial lectins. Compared with a reference monovalent sugar residue, the glycoclusters showed superior binding to lectins due to the multivalent bonding. With an appropriate length spacer between the sugar residues and the pillar[5]arene core, the glycoclusters showed higher affinity to lectins. The same group also synthesised hetero-glycoclusters containing two different sugar residues (e.g., galactoses and fucoses) based on a [2]rotaxane scaffold.<sup>42</sup> To achieve this, one sugar residue was used as a stopper and a [2]rotaxane was produced using a CuAAC reaction. Then, another CuAAC reaction between the azide-functionalised pillar[5]arene ring in the [2]rotaxane and the other sugar residue afforded the hetero-glycoclusters. Because these [2]rotaxanes contained two different sugars, they showed multivalent binding to two different bacterial lectins.

## Water-soluble deep-cavity cavitands

### Preamble

The definition of deep-cavity cavitands used here are resorcin[4]arene-based hosts where an additional second row of (normally aromatic) rings has been added to the resorcinarene. The second row – added either as a bridge between adjacent resorcinol hydroxyl groups or to the 2-position of the resorcinol rings themselves – deepens the binding pocket significantly.

Examples of the latter were first to appear in the literature, but extending the cavity of these hosts using suitable bridging moieties has proven to be the most popular.

The gross structural difference between deep-cavity cavitands and cucurbiturils or pillarenes is that cavitands are bowl-shaped rather than toroidal; they are closed at one end. This has manifold implications. For example, solvation of the pocket is harder, and hence the pocket can be viewed as more hydrophobic. Relatedly, replacing water in a pocket with a guest via an associative ( $S_N2$ -like) mechanism is difficult with only one portal in or out; dissociative ( $S_N1$ -like) mechanisms dominate. Moreover, the  $C_{nv}$  symmetry and more encompassing structures of cavitands lead to considerable control of guest orientation and conformation (binding motif). As we will discuss, this control has considerable ramifications regarding the applications of cavitands. Finally, on the topic of general shape, it is also important to note that by careful design, cavitands have also proven adept at undergoing self-assembly to form all-encapsulating containers; containers that take all of the aforementioned points to the extreme.

Two examples of the first water soluble deep-cavity cavitands are **1** and **2** (Fig. 17) that are described in more detail in these reviews.<sup>43, 44</sup> Cavitand **1** reported by the Reinhoudt group possesses four pyridinium groups at the upper rim. Cavitands with longer pendent R groups proved to be more water-soluble because of efficient aggregation. The non-aggregating cavitand with methyl pendent groups (or feet) was shown to form weak, fast exchanging 1:1 complexes with small aromatic guests. A similar strategy was used to give the ethylene-bridged host **2** reported by Diederich. With a more preorganized cavity this host formed 1:2 host-guest complexes in pure water and 1:1 host-guest complexes in buffer. Guests such as adenosine triphosphate that associated via electrostatic interactions and the Hydrophobic Effect were found to bind strongly to **2**.

### Deep-cavity Cavitands via bridging strategies

Extending the cavity walls of resorcinarenes using the bridges between resorcinol moieties has to date proven to be more popular. Within this approach two general classes of cavitands have emerged: velcrands and benzal-bridged cavitands.<sup>43, 45, 46</sup> The two most studied water-soluble velcrands are those with benzimidazoles (**3**) and benzimidazolones (**4**) bridges. A key structure feature of velcrands is that they exist as an equilibrium mixture of two conformations: a flattened ( $C_{2v}$ ) kite form that has a strong predisposition to dimerize in solution, and a deeper concave ( $C_{4v}$ ) vase form capable of binding guests. This equilibrium between the vase and kite forms is largely controlled by the precise nature of the host and solvent, and if present, the nature of the guest. In many of the studies in water these velcrands exist as a kite-form complex containing one strongly binding tetrahydrofuran molecule; a residual solvent molecule from the synthesis of the host.

In 2004, the Gibb group reported the first water-soluble benzal bridged type cavitand **5a** (Fig. 17).<sup>45</sup> The so-called “octa-acid” (OA) **5a**, is sparingly soluble at neutral aqueous solution, but highly soluble and monomeric at  $\text{pH} > 7$ . This host possesses a  $\sim 0.8$  nm wide  $\times$   $\sim 0.8$  nm deep hydrophobic pocket that, like a velcrand is closed off at the base, but is more preorganized. The evenly spread charges on the surface of this host bestow it with excellent behaviour in aqueous solution. Other variations on this general structure have subsequently



been reported. For example, *tetra*-exo-methyl octa acid (TEMOA) **5b** possesses a slightly differently shaped hydrophobic pocket. Moreover, cationic water-soluble cavitands such as **5c** and **5d** have also been reported, as have neutral hosts that utilize dendritic or polymeric coats to attain water-solubility.<sup>45</sup> To date these types of cavitands have been shown to form 1:1 complexes, as well as undergo self-assembly to form a range of complexes: 2:1, 2:2, 4:2 and 6:3.

### 1:1 host-guest complexes: controlling guest reactivity

The  $C_{nv}$  symmetry of cavitands can lead to specific bound guest orientations. Using  $^1\text{H}$ -NMR the Gibb group observed this in the 1:1 complexes between aliphatic carboxylates and OA **5a**; the guests buried their hydrophobic tails in the pocket of **5a**, and placed their polar carboxylate head group exposed to the aqueous medium.<sup>45</sup> This additional charged group on the surface of the complex suppresses any host assembly (*vide infra*). Isothermal Titration Calorimetry (ITC) showed that the affinity between OA and these guests were generally stronger than the corresponding affinities with similarly sized  $\beta$ -cyclodextrin. For example, the respective affinities between OA and  $\beta$ -cyclodextrin with adamantane carboxylate are  $K_a = 1.14 \times 10^6$  and  $1.05 \times 10^5 \text{ M}^{-1}$ .<sup>45</sup> This is tentatively ascribed to a combination of the more encapsulating pocket of OA **5a** being relatively poorly hydrated, and it being able to form more non-covalent contacts with the guest. These types of complexes with amphiphiles have proven useful in predictive blind challenges for computational chemist testing their modelling strategies.<sup>47</sup>

Even hydrated anions such as  $\text{I}^-$  or  $\text{ClO}_4^-$  have an affinity with OA **5a**, and such complexation events have been shown to attenuate the binding of non-polar guests by a simple competition mechanism. Moreover, this competition has been shown to replicate the salting-in phenomenon of the Hofmeister effect.<sup>48</sup> This relatively strong anion affinity can again be ascribed to the true concavity of **5a**.

Interestingly, although a guest dissociative ( $S_N1$ -like) mechanism is assumed to operate with these 1:1 complexes, a different mechanism seems to be in operation when the guest being replaced is water. Thus, in silico studies have demonstrated that if a hydrophobic guest approaches within 3–4 Å of the pocket portal of **5a** it disrupts stabilizing hydrogen bonds between bound and bulk water.<sup>49</sup> At a longer distance this initially leads to fluctuations in the water density in the pocket, but as the guest approaches to  $\sim 3$  Å it ultimately leads to complete dehydration of the binding site. Thus water displacement by a guest follows a triggered dissociation mechanism.

Velcrand **3** has been shown to form 1:1 complexes with tetraalkylammonium salts.<sup>46</sup> In this case the guest is again aligned in one specific orientation; with the larger alkyl group buried and the ammonium group at the portal of the host where it can interact with water and the carboxylates of the host.

The driving force of the hydrophobic effect, combined with the fact that these hosts only have one portal, means that it is possible to compress flexible guests into unnaturally small spaces.<sup>43, 46</sup> Consider for example how host **3** binds two surfactants, sodium dodecylsulfate and dodecyl phosphatidylcholine, in a 1:1 manner. Free in non-aqueous media, alkyl chains

favor extended (*anti*) conformations to minimize steric interactions and maximize surface area. Such an extended conformation is energetically unfavorable in water, and consequently when presented with the cavity of **3** the alkyl groups of these guests compact themselves so as to minimize their exposure to bulk water and maximize their contacts with the host. In short, they coil into helices inside the cavity (Fig. 18).

The truly concave nature of deep-cavity cavitands can also induce guests to preferentially adopt U- or J-shaped conformations or motifs. In a recent example, N-methylated benzimidazolones bridged cavitand **4b** was shown to bind amphiphilic guests such as n-alcohols in a folded confirmation, where the hydroxyl group is located at the rim or portal and the hydrophobic chains are deeply buried into the pocket. For guest such as C8 and C9, the chain is extended, but with longer guests (greater than C10) the chain forms a reverse turn (Fig 19). Consequently, the longest guests adopt J-shaped motifs anchored as such by the preference of the polar head group to remain solvated.<sup>46</sup> In contrast, all examples of  $\alpha,\omega$ -diol guest examined were shown to bind in folded, U-shaped motifs.

The observation that guests can be folded into conformations whereby the termini are pushed closely together raises the prospect of being able to bring about controlled macrocyclization processes. Two examples with host **4a** include the enhanced cyclization of  $\omega$ -amino acids to form lactams, and the formation of di-lactams.<sup>50</sup> In the latter example, long-chain diamines were first complexed to **4a** before the addition of the di-*N*-hydroxysuccinimide ester of succinic acid resulted in the rapid formation of the corresponding 17- to 25-membered dilactams (Fig. 20).

Very recently, host **4b** was also shown to engender unusual reactions of bound guests. For example, bound diesters were shown to form 1:1 complexes in which the guest rapidly alternatives between two identical J-shaped conformations via a “yo-yo” motion (Fig. 21).<sup>51</sup> Under acidic conditions, one ester group of the guest is hydrolyzed ~10 times faster than in bulk solution, i.e., the host catalyzes hydrolysis, and this results in the guest adopting a fixed motif with the carboxylic acid group at the head of the J-motif and the remaining ester at the short tail of the motif buried in the binding pocket. As a result, the hydrolysis of the second ester is attenuated 2–4 times. Hydrolysis under basic conditions (saponification) gave much better yields of monoester. Evidently, the anchoring of the carboxylate at the head of the J-motif and exposed to bulk solution is much stronger than the anchoring properties of the carboxylate formed under acidic conditions. Other recent examples of controlling guest reactivity with **4b** include biasing Staudinger reduction of  $\alpha,\omega$ -diazides, and converting  $\alpha,\omega$ -diisocyanates to aminoisocyanates.<sup>51</sup>

### Encapsulation and Self-Assembly

The unusual guest encompassing properties of bowl-shaped hosts can be taken one step further by self-assembly. Thus, dimerization of these hosts leads to a completely integral inner space for total guest encapsulation. As we describe, the dry, yocto-liter inner spaces of such containers – or put another way the compartmentalization brought about by such supramolecular hosts – have considerable potential to control unique reactions or engender novel separation protocols.

Host OA (**5a**) and its *tetra-endo*-methyl derivative TEMOA (**5b**) assemble via the Hydrophobic Effect. As a result, even though the encapsulation complexes are held together by relatively weak interactions (aromatic stacking between the hosts and C–H... $\pi$  interactions between the hosts and guest or guests) binding is strong. For example, of the steroids first investigated binding to the dimer of **5a**, (+)-dehydroisoandrosterone was shown by  $^1\text{H-NMR}$  to have a minimum association constant  $1 \times 10^8 \text{ M}^{-1}$ .<sup>45</sup> This indirect driving of assembly rooted in the cohesive forces between water molecules means that even small alkanes form very stable 2:2 host-guest complexes with **5a**.<sup>52</sup> With larger alkanes (C11–C14) helical motifs are observed for the bond guest, whilst for even still larger guests (C18–C23) U-shape motifs have been identified by  $^1\text{H-NMR}$  (Fig. 22). For this dimer host the limit for *n*-alkane guest binding is approximately C24–C26, at which point the center of the guest begins to separate the two hemispheres of the capsule.

With four *endo*-methyl groups on the top of the cavitand, TMEOA **5b** has a slightly deeper cavity but a narrower portal compared to OA **5a**. This leads to very different assembly and complexation profiles. For example, the complexes between **5b** and the series of *n*-alkane guests C1 through C14 are: 1:1 for C1, C2, C7 and C8, 2:2 for C5, and 2:1 for C9–C14. Guests C3, C4 and C6 form mixtures of 1:1 and 2:2 complexes. These host-guest systems therefore function as a nine-input, one-output logic gate.<sup>53</sup> Interestingly, this non-monotonic assembly profile is reflected in the predisposition of TEMOA **5b** to form hetero-host guest encapsulation complexes with OA **5a** (**5a.5b.guest**).<sup>45</sup>

Octa-acid host **5a** has only been observed to form a dimeric container. However, this is not the case with TEMOA **5b**. The aforementioned complex assembly profile of **5b** is in fact a reflection of its reduced propensity to dimerize; the methyl groups ( $\text{R}'$  in Fig 17) sterically interfere in the dimerization interface between the two hosts. However, they do not interfere in the assembly of larger assemblies. Thus, with *n*-alkane chains C17–C20 **5b** forms mono-dispersed, pseudo  $T_d$  ( $D_{2d}$ ) 4:2 host-guest complexes, whilst for C24–C26 guests nonary 6:3 host-guest complexes with overall  $O_h$  symmetry are formed (Fig. 23).<sup>45</sup> Although  $^1\text{H-NMR}$  did not reveal the precise binding motifs of the bound guests in these complexes, these are the most capacious hosts assembled in water, respectively defining 1400–1500 and 3200–3700  $\text{\AA}^3$ .

Recently, the Rebek group has extended their study of capsular complexes to the aqueous phase. For example, host **4a** has been shown to undergo self-assembly in water around a range of stilbenes, paraquats, and related derivatives.<sup>46</sup>

### Separations with Capsules

Capsule **5a<sub>2</sub>** has been used to bring about both physical separations and kinetic resolutions. An example of the former is shown in Fig 24.<sup>54</sup> Briefly, the addition of a mixture of hydrocarbon gases to the head-space above a solution of the host leads to the selective sequestration of the strongest binding alkane. The well-defined structure of the supramolecular host leads to selectivity at the methylene group level. Thus, with a mixture of propane and butane only two molecules of the later are sequestered within the host leaving an enriched or pure sample of propane in the head-space.

Capsule **5a**<sub>2</sub> can also be used to bring about the kinetic resolution of constitutional isomeric of esters by selective protection (Fig. 25).<sup>55</sup> In the absence of the host, the selected C<sub>11</sub>H<sub>22</sub>O<sub>2</sub> guests undergo saponification at rates commensurate with the size of their alkoxy group. However, in the presence of **5a**<sub>2</sub> these intrinsic hydrolyses were strongly modulated by the relative affinity each ester has for the capsule. As shown in Fig 25, when methyl decanoate and ethyl nonanoate are saponified in the presence of **5a** only 18% of the former is hydrolyzed in the time it takes to hydrolyze all of the latter. A detailed analysis involving  $K_a$  and rate determinations allowed a Michaelis-Menton type model to be built that fitted the observed resolutions. Briefly, the more strongly bound ester was protected within the capsule which greatly retarded its hydrolysis relative to the weaker binding competitor.

### Reactions in capsules

Many examples of how the capsule formed by **5a** controls the photochemistry and photophysics of encapsulated guests have been reported.<sup>56</sup> One interesting study involved the comparison of a series of  $\alpha$ -(*n*-alkyl)-dibenzyl ketones (DBKs). All DBK guests formed 2:1 host/guest complexes with the dimer of OA **5a**, but within the series three different packing motifs were formed depending on the length of the side chain. For the small R groups (R = Me, Et, *n*-propyl), each phenyl ring of the guest occupied the polar regions of the host while the R group filled the equatorial region (Fig. 26 illustrates this with the methyl guest). For mid-sized R groups (R = *n*-butyl, *n*-pentyl and *n*-hexyl) it was found that one phenyl ring and the R group occupied the polar regions of the host and the proximal phenyl ring (red in Fig. 26) filled the equatorial region. Finally, in the case of the largest R groups (R = *n*-heptyl and *n*-octyl), the guest packed the cavity such that the distal phenyl ring (blue in Fig. 26) occupies the equatorial region of the capsule. Each of these motifs led to different photochemical outcomes, with the smaller or mid-sized alkyl chains lead to Norrish type I products and the long alkyl chains lead to Norrish type II products. Many of the rearrangement products, e.g. the benzyl-phenylketones, are not seen in solution. Instead they arose through exceedingly strong cage effects and the non-covalent interactions between the host and the intermediate radicals. Another example is the photochemical selective oxidation of olefins by singlet oxygen within the **5a**<sub>2</sub> capsule.<sup>56</sup> Normally, the addition of singlet oxygen to the double bond of alkenes possessing multiple allylic positions leads to a mixture of allylic hydro-peroxides. However, 1-methyl cyclohexenes formed a 2:2 host- guest complex in which the guests adopt specific orientations with the methyl group of each anchored into one pole of the capsule. This leaves only the C-3 position accessible via partial opening of the capsule. With singlet oxygen generated from the irradiation of dimethyl benzyl (DMB) encapsulated in the same type of capsule, and “communication” between the two capsular complexes, allylic substrates were selectively oxidized in up to 95% yield (Fig. 27).

### Conclusions

This tutorial review has highlighted select, preeminent examples from the growing fields of cucurbiturils, pillarenes and cavitands. Studies with these hosts are revealing new and unusual properties arising from their ability to efficiently sequester guest molecules from the surrounding aqueous solution. At the same time, these studies are revealing details about the

links between solvation of small spaces and the Hydrophobic Effect, and how anion affinity for non-polar surfaces is implicated in the Hofmeister effect. On both fronts, there is evidently much to explore and much to do; further studies can be expected to demonstrate a further broadening of the range of properties demonstrated by these hosts, and more details concerning the dissolution of solutes in water.

## Acknowledgments

K.K and J.M. gratefully appreciate the financial support from the Institute for Basic Science (IBS) [IBS-R007-D1] of the Republic of Korea. T.O. gratefully appreciates the financial support from JSPS KAKENHI Grant Numbers 15H00990, 16H04130 and Kanazawa University CHOZEN Project. B.C.G. and W.Y. thank the National Institutions of Health for financial support (GM 098141).

## Notes and references

1. Chandler D. *Nature*. 2007; 445:831–832. [PubMed: 17314967]
2. Jungwirth P, Cremer PS. *Nat Chem*. 2014; 6:261–263. [PubMed: 24651180]
3. Ball P. *Chem Rev*. 2008; 108:74–108. [PubMed: 18095715]
4. Ben-Amotz D. *Annu Rev Phys Chem*. 2016; 67:617–638. [PubMed: 27215821]
5. Hillyer MB, Gibb BC. *Annu Rev Phys Chem*. 2016; 67:307–329. [PubMed: 27215816]
6. Lee JW, Samal S, Selvapalam N, Kim HJ, Kim K. *Acc Chem Res*. 2003; 36:621–630. and references therein. [PubMed: 12924959]
7. Kim J, Jung IS, Kim SY, Lee E, Kang JK, Sakamoto S, Yamaguchi K, Kim K. *J Am Chem Soc*. 2000; 122:540–541.
8. Day A, Arnold AP, Blanch RJ, Snushall B. *J Org Chem*. 2001; 66:8094–8100. [PubMed: 11722210]
9. Li Q, Qiu SC, Zhang J, Chen K, Huang Y, Xiao X, Zhang Y, Li F, Zhang YQ, Xue SF, Zhu QJ, Tao Z, Lindoy LF, Wei G. *Org Lett*. 2016; 18:4020–4023. [PubMed: 27499014]
10. Lagona J, Mukhopadhyay P, Chakrabarti S, Isaacs L. *Angew Chem Int Ed Engl*. 2005; 44:4844–4870. and references therein. [PubMed: 16052668]
11. Shetty D, Khedkar JK, Park KM, Kim K. *Chem Soc Rev*. 2015; 44:8747–8761. and references therein. [PubMed: 26434388]
12. Barrow SJ, Kasera S, Rowland MJ, del Barrio J, Scherman OA. *Chem Rev*. 2015; 115:12320–12406. and references therein. [PubMed: 26566008]
13. Assaf KI, Nau WM. *Chem Soc Rev*. 2015; 44:394–418. and references therein. [PubMed: 25317670]
14. Isaacs L. *Acc Chem Res*. 2014; 47:2052–2062. and references therein. [PubMed: 24785941]
15. Kim HJ, Heo J, Jeon WS, Lee E, Kim J, Sakamoto S, Yamaguchi K, Kim K. *Angew Chem Int Ed Engl*. 2001; 40:1526–1529. [PubMed: 11317324]
16. Ko YH, Kim E, Hwang I, Kim K. *Chem Commun*. 2007:1305–1315. and references therein.
17. Liu J, Lan Y, Yu Z, Tan CS, Parker RM, Abell C, Scherman OA. *Acc Chem Res*. 2017; 50:208–217. [PubMed: 28075551]
18. Yang H, Yuan B, Zhang X, Scherman OA. *Acc Chem Res*. 2014; 47:2106–2115. and references therein. [PubMed: 24766328]
19. Liu S, Ruspic C, Mukhopadhyay P, Chakrabarti S, Zavalij PY, Isaacs L. *J Am Chem Soc*. 2005; 127:15959–15967. [PubMed: 16277540]
20. Jeon WS, Moon K, Park SH, Chun H, Ko YH, Lee JY, Lee ES, Samal S, Selvapalam N, Rekharsky MV, Sindelar V, Sobransingh D, Inoue Y, Kaifer AE, Kim K. *J Am Chem Soc*. 2005; 127:12984–12989. [PubMed: 16159293]
21. Rekharsky MV, Mori T, Yang C, Ko YH, Selvapalam N, Kim H, Sobransingh D, Kaifer AE, Liu S, Isaacs L, Chen W, Moghaddam S, Gilson MK, Kim K, Inoue Y. *Proc Natl Acad Sci U S A*. 2007; 104:20737–20742. [PubMed: 18093926]

22. Cao L, Sekutor M, Zavalij PY, Mlinaric-Majerski K, Glaser R, Isaacs L. *Angew Chem Int Ed Engl.* 2014; 53:988–993. [PubMed: 24382654]
23. Chodera JD, Mobley DL. *Annu Rev Biophys.* 2013; 42:121–142. [PubMed: 23654303]
24. Biedermann F, Nau WM, Schneider HJ. *Angew Chem Int Ed Engl.* 2014; 53:11158–11171. and references therein. [PubMed: 25070083]
25. Ogoshi T, Kanai S, Fujinami S, Yamagishi TA, Nakamoto Y. *J Am Chem Soc.* 2008; 130:5022–5023. [PubMed: 18357989]
26. Ogoshi T, Yamagishi TA, Nakamoto Y. *Chem Rev.* 2016; 116:7937–8002. [PubMed: 27337002]
27. Xue M, Yang Y, Chi X, Zhang Z, Huang F. *Acc Chem Res.* 2012; 45:1294–1308. [PubMed: 22551015]
28. Strutt NL, Zhang H, Schneebeli ST, Stoddart JF. *Acc Chem Res.* 2014; 47:2631–2642. [PubMed: 24999824]
29. Wu X, Gao L, Hu XY, Wang L. *Chem Rec.* 2016; 16:1216–1227. [PubMed: 27061964]
30. Wang Y, Ping G, Li C. *Chem Commun.* 2016; 52:9858–9872.
31. Ogoshi T, Hashizume M, Yamagishi TA, Nakamoto Y. *Chem Commun.* 2010; 46:3708–3710.
32. Li C, Ma J, Zhao L, Zhang Y, Yu Y, Shu X, Li J, Jia X. *Chem Commun.* 2013; 49:1924–1926.
33. Yu G, Xue M, Zhang Z, Li J, Han C, Huang F. *J Am Chem Soc.* 2012; 134:13248–13251. [PubMed: 22827832]
34. Ma Y, Ji X, Xiang F, Chi X, Han C, He J, Abliz Z, Chen W, Huang F. *Chem Commun.* 2011; 47:12340–12342.
35. Ogoshi T, Kida K, Yamagishi TA. *J Am Chem Soc.* 2012; 134:20146–20150. [PubMed: 23163776]
36. Chang Y, Yang K, Wei P, Huang S, Pei Y, Zhao W, Pei Z. *Angew Chem Int Ed Engl.* 2014; 53:13126–13130. [PubMed: 25267331]
37. Hu XB, Chen Z, Tang G, Hou JL, Li ZT. *J Am Chem Soc.* 2012; 134:8384–8387. [PubMed: 22574988]
38. Ogoshi T, Takashima S, Yamagishi TA. *J Am Chem Soc.* 2015; 137:10962–10964. [PubMed: 26270554]
39. Ni M, Zhang N, Xia W, Wu X, Yao C, Liu X, Hu XY, Lin C, Wang L. *J Am Chem Soc.* 2016; 138:6643–6649. [PubMed: 27159331]
40. Yu G, Jie K, Huang F. *Chem Rev.* 2015; 115:7240–7303. [PubMed: 25716119]
41. Buffet K, Nierengarten I, Galanos N, Gillon E, Holler M, Imberty A, Matthews SE, Vidal S, Vincent SP, Nierengarten JF. *Chemistry.* 2016; 22:2955–2963. [PubMed: 26845383]
42. Vincent SP, Buffet K, Nierengarten I, Imberty A, Nierengarten JF. *Chemistry.* 2016; 22:88–92. [PubMed: 26467313]
43. Biroš SM, Rebek J Jr. *Chem Soc Rev.* 2007; 36:93–104. and references therein. [PubMed: 17173148]
44. Oshovsky GV, Reinhoudt DN, Verboom W. *Angew Chem Int Ed Engl.* 2007; 46:2366–2393. and references therein. [PubMed: 17370285]
45. Jordan JH, Gibb BC. *Chem Soc Rev.* 2015; 44:547–585. and references therein. [PubMed: 25088697]
46. Mosca S, Yu Y, Rebek J Jr. *Nat Protoc.* 2016; 11:1371–1387. and references therein. [PubMed: 27388554]
47. Gallicchio E, Chen H, Chen H, Fitzgerald M, Gao Y, He P, Kalyanikar M, Kao C, Lu B, Niu Y, Pethe M, Zhu J, Levy RM. *J Comput Aided Mol Des.* 2015; 29:315–325. [PubMed: 25726024]
48. Sokkalingam P, Shraberg J, Rick SW, Gibb BC. *J Am Chem Soc.* 2016; 138:48–51. [PubMed: 26702712]
49. Ewell J, Gibb BC, Rick SW. *J Phys Chem B.* 2008; 112:10272–10279. [PubMed: 18661937]
50. Shi Q, Masseroni D, Rebek J. *J Am Chem Soc.* 2016; 138:10846–10848. and references therein. [PubMed: 27529442]
51. Shi Q, Mower MP, Blackmond DG, Rebek J Jr. *Proc Natl Acad Sci U S A.* 2016; 113:9199–9203. and references therein. [PubMed: 27482089]



52. Liu S, Russell DH, Zinnel NF, Gibb BC. *J Am Chem Soc.* 2013; 135:4314–4324. [PubMed: 23448338]
53. Gan H, Benjamin CJ, Gibb BC. *J Am Chem Soc.* 2011; 133:4770–4773. [PubMed: 21401093]
54. Gibb CLD, Gibb BC. *J Am Chem Soc.* 2006; 128:16498–16499. [PubMed: 17177388]
55. Liu S, Gan H, Hermann AT, Rick SW, Gibb BC. *Nat Chem.* 2010; 2:847–852. [PubMed: 20861900]
56. Ramamurthy V. *Acc Chem Res.* 2015; 48:2904–2917. and references therein. [PubMed: 26488308]

## Biographies



**James Murray** studied medicinal chemistry at the University of Leeds (MChem, 2010) and received a Ph.D. from the same institution, working on self-assembled monolayers (2014). After one year as a research associate in chemical proteomics at Newcastle University (UK) he joined the Center for Self-assembly of Complexity in 2016, where his research interests are in the applications of supramolecular chemistry to chemical biology.

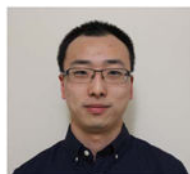


**Kimoon Kim** studied chemistry at SNU (B.S., 1976), Korea Advanced Institute of Science and Technology (M.S., 1978), and Stanford University (Ph.D., 1986). After two-years of postdoctoral work at Northwestern University, he joined POSTECH where he is now a Distinguished University Professor. Recently, he has been appointed as director of CSC, IBS. His current research focuses on developing novel functional materials and systems based on supramolecular chemistry.



**Bruce C. Gibb** received both his B.Sc. (1987) and Ph.D. (1992) degrees from Robert Gordon's University, where his director of studies for his doctoral degree was Philip J. Cox. He then carried out post-doctoral research at the University of British Columbia with John C. Sherman and subsequently at New York University with James W. Canary. In 1996 he

joined the University of New Orleans, where he was promoted to associate professor in 2002, full professor in 2005, and ultimately University Research Professor in 2007. In 2012 he moved to Tulane University. His research interests focus on the many aspects of aqueous supramolecular chemistry.



**Wei Yao** was born and raised in Xi'an, China. He obtained his BS in Pharmacy and MS in Medicinal Chemistry from China Pharmaceutical University. In 2014, he moved to Tulane University (New Orleans, USA) to pursue his PhD degree in organic chemistry in professor Gibb's research group. Currently, his research focuses on two topics: Hofmeister ion binding to synthetic hosts, and proteins, and the designing and synthesis of functionalized water-soluble cavitands for supramolecular polymers.



**Tomoki Ogoshi** received his B.S. (2000), M.S. (2002), and Ph.D. degrees (2005) from Kyoto University under the supervision of Prof. Yoshiki Chujo. He was a JSPS postdoctoral research fellow (2005–2006) in the Graduate School of Science at Osaka University in the group of Prof. Akira Harada. In 2006, he moved to the Graduate School of Natural Science and Technology at Kanazawa University as an assistant professor (2006–2010). He was an associate professor (2010–2015) and was promoted to a professor at the same university at 2015. He works also as JST-PRESTO Researcher: PRESTO program “Hyper-nano-space design toward innovative functionality” from Oct. 2013 under the research supervisor of Prof. Kazuyuki Kuroda (Waseda University). He has received HGCS Japan Award Excellence 2010 (2011), The Chemical Society of Japan Award for Young Chemists (2012), The Cram Lehn Pedersen Prize in Supramolecular Chemistry; Royal Society of Chemistry (2013), The Commendation for Science and Technology by the Minister of Education, Culture, Sports, Science and Technology (2014), Nozoe Memorial Award for Young Organic Chemists (2016), Banyu Chemist Award 2016 (2016) and Lectureship Award MBLA 2016 (2017). His research interests include organic synthesis, and supramolecular and hybrid materials.

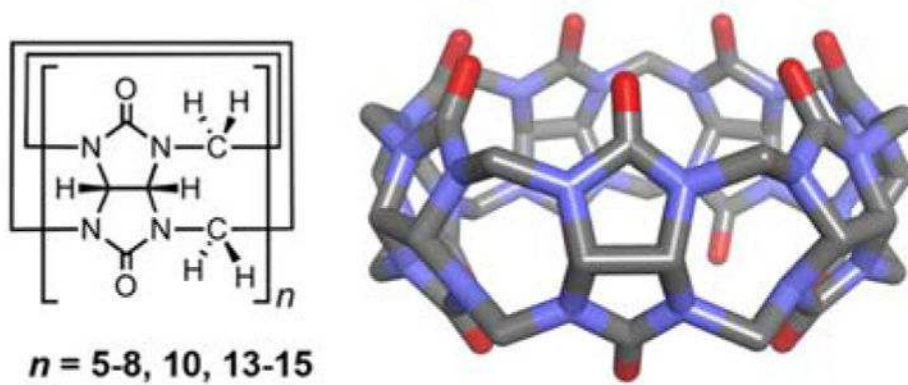


**Fig. 1.** The chemical structures of the known CB[n] and a stick representation of CB[7].

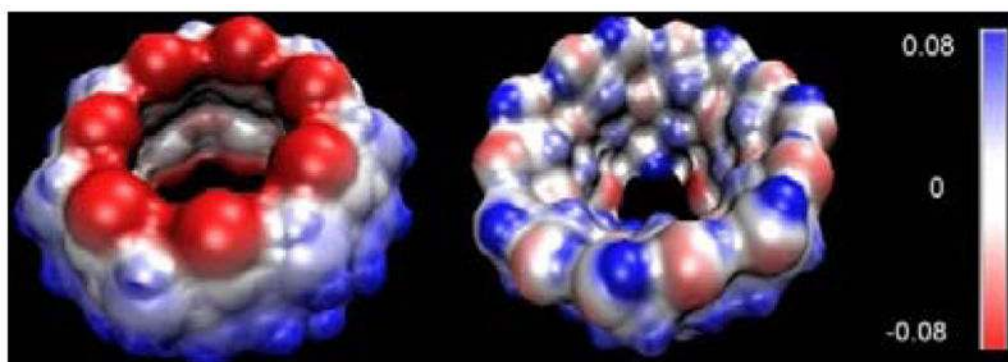


**Fig. 2.** The surface electrostatic potential for CB[7] (left) and  $\beta$ -cyclodextrin (right). The blue colour represents positive charge, and the red represents negative. Taken from Ref. 11. Copyright, 2015 Royal Society of Chemistry.

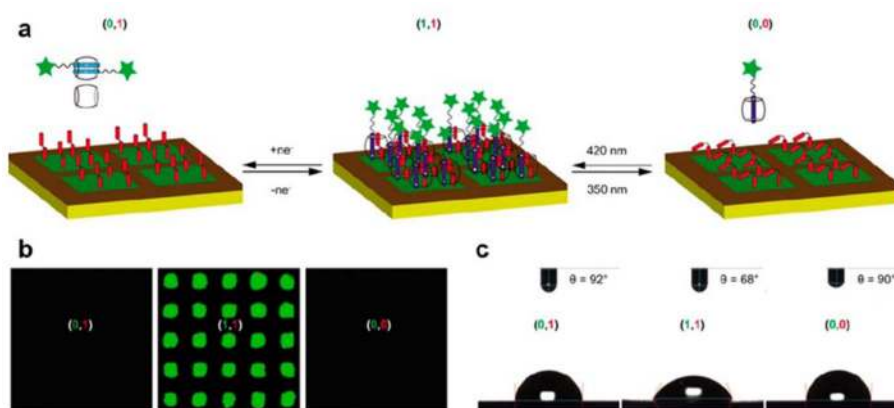
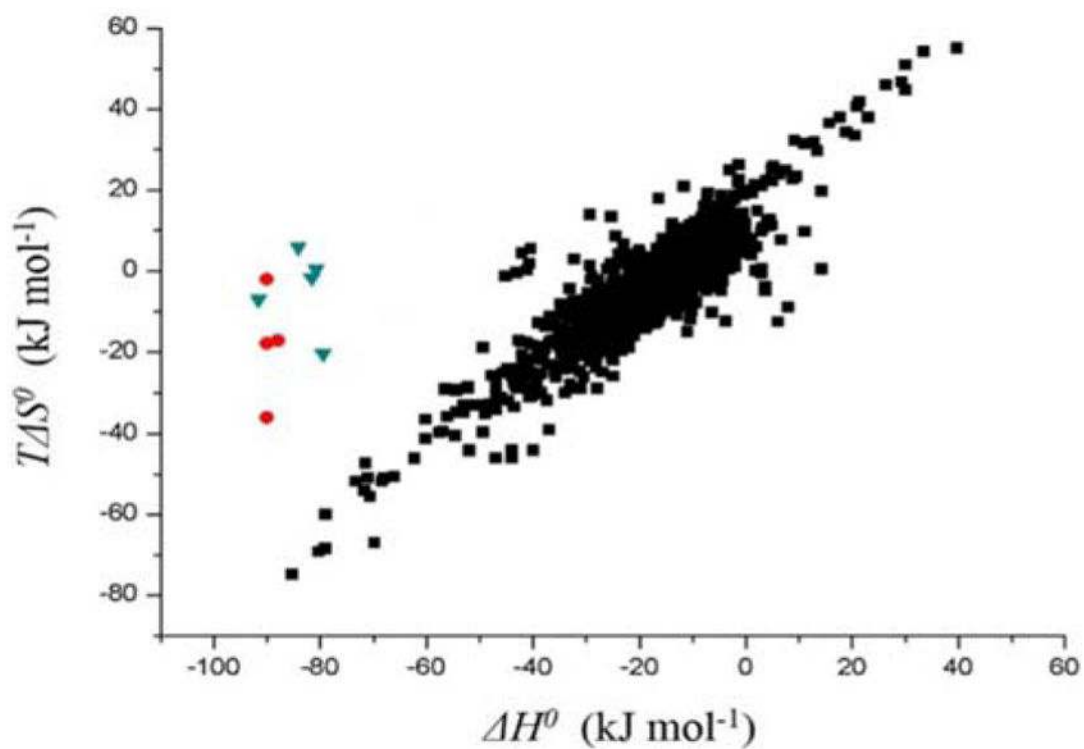


**Fig. 3.** a) Orthogonal stimuli-responsive biointerfaces on the base of CB[8]-mediated ternary host-guest complex; (b) fluorescence microscopy images and (c) water contact angle measurement of the corresponding states. Reprinted with permission from *Nat. Commun.* 2012, **3**, 1207. Copyright 2012 Nature Publishing Group.

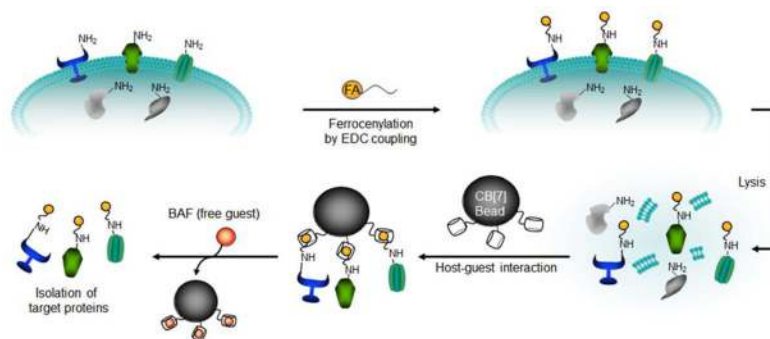
A		K (M <sup>-1</sup> )	$\Delta H^{\circ}_{\text{expt}}$ [kcal mol <sup>-1</sup> ]	$-\Delta S^{\circ}_{\text{expt}}$ [kcal mol <sup>-1</sup> ]
Guests F1-F4				
		$(3.2 \pm 0.5) \times 10^9$	$-21.5 \pm 0.5$	$8.6 \pm 0.5$
		$(2.4 \pm 0.8) \times 10^{12}$	$-21.0 \pm 0.5$	$4.1 \pm 0.5$
		$(4.1 \pm 1.0) \times 10^{12}$	$-21.5 \pm 0.5$	$4.3 \pm 0.4$
		$(3.0 \pm 1.0) \times 10^{15}$	$-21.5 \pm 0.2$	$0.5 \pm 0.5$
B		K (M <sup>-1</sup> )	$\Delta H^{\circ}_{\text{expt}}$ [kcal mol <sup>-1</sup> ]	$-\Delta S^{\circ}_{\text{expt}}$ [kcal mol <sup>-1</sup> ]
Guests A1-A5				
		$(2.3 \pm 0.8) \times 10^{10}$	$-19.0 \pm 0.4$	$4.9 \pm 0.4$
		$(1.7 \pm 0.8) \times 10^{14}$	$-19.3 \pm 0.4$	$-0.1 \pm 0.5$
		$7.7 \times 10^{14}$	$-21.9 \pm 0.4$	1.7
		$5 \times 10^{15}$	$-20.1 \pm 0.4$	-1.4
		$(1.0 \pm 0.3) \times 10^{14}$	$-19.5 \pm 0.4$	$0.4 \pm 0.5$
C				
Guests D1-D3				
K (M <sup>-1</sup> )		$4.0 \times 10^9$	$(1.4 \pm 0.3) \times 10^{11}$	$7.2 \times 10^{17}$

**Fig. 4.** High affinity CB[7] guests and their thermodynamic parameters. A: Ferrocene derivatives; B: adamantane derivatives; and C: The record-breaking diamantane high affinity guests. All of the binding affinities were measured in water, with the exception of D1–D3, which were measured in NaO<sub>2</sub>CCD<sub>3</sub>, pH = 4.74. Adapted from Ref. 11.

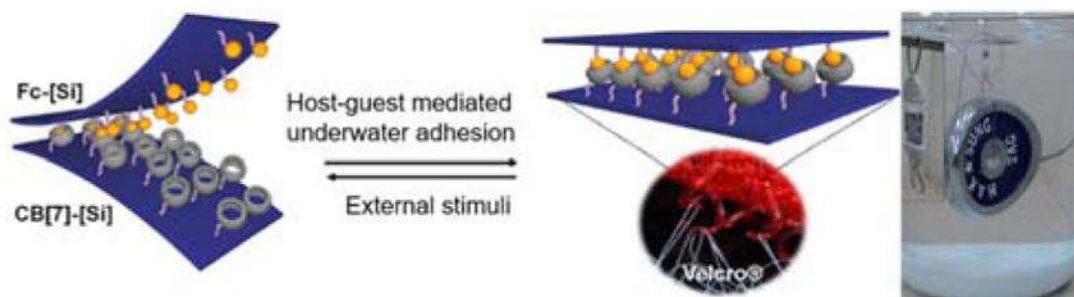




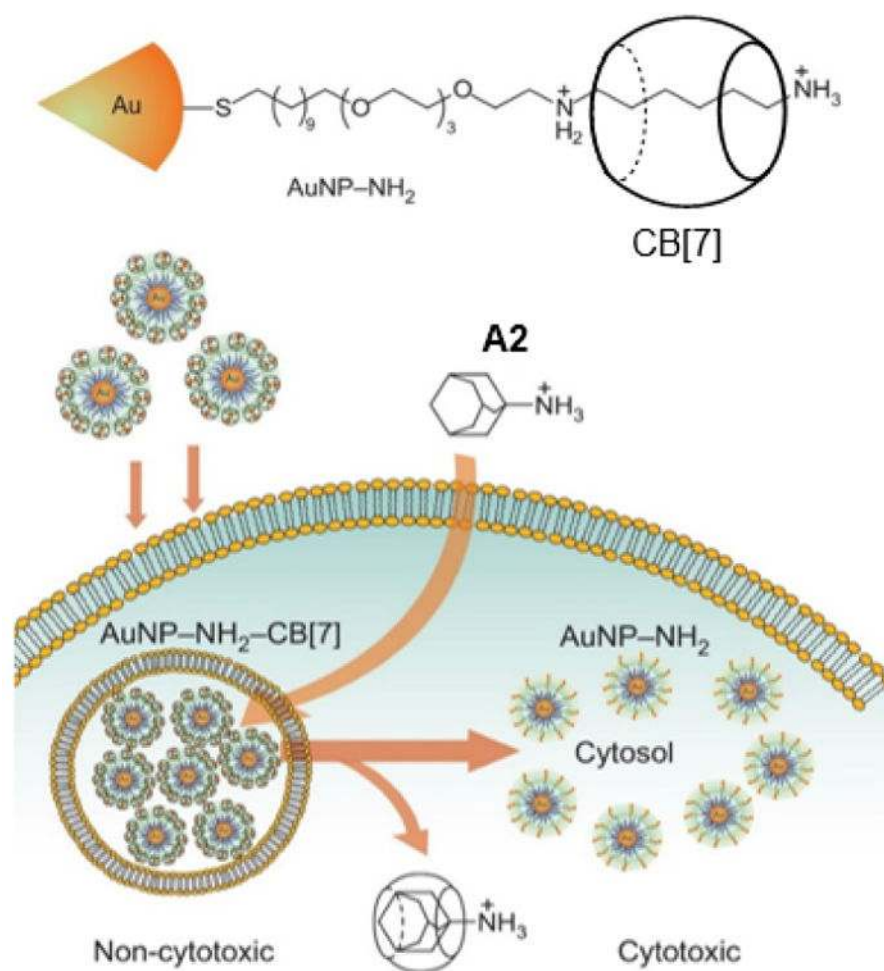
**Fig. 5.** The thermodynamic data for the complexation of ferrocene (●) and adamantane (▼) derivatives to CB[7] compared with cyclodextrin-guest complexation(■). The data points for the high affinity CB[7] guests are significantly deviated from those of the cyclodextrin guests. Modified from Ref. 11. Copyright, 2015 Royal Society of Chemistry



**Fig. 6.** The isolation of plasma membrane protein by use of CB[7] immobilized onto a support bead. The captured proteins are released by exchange with a higher affinity guest, BAF (**F4**). Reprinted with permission from *Nat. Chem.* 2011, **3**, 154–159. Copyright 2011, Nature Publishing Group



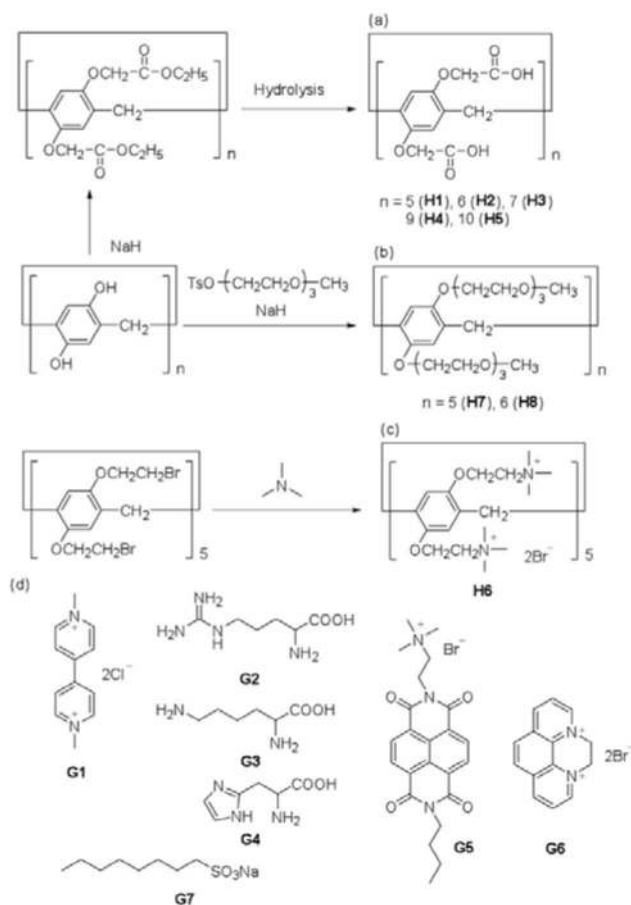
**Fig. 7.** Supramolecular Velcro<sup>®</sup> for underwater adhesion between CB[7] and Fc functionalized surfaces. Reprinted with permission from *Angew. Chem., Int. Ed.*, 2013, **52**, 3140–3144. Copyright 2013, Wiley-VCH Verlag GmbH & Co. KGaA.



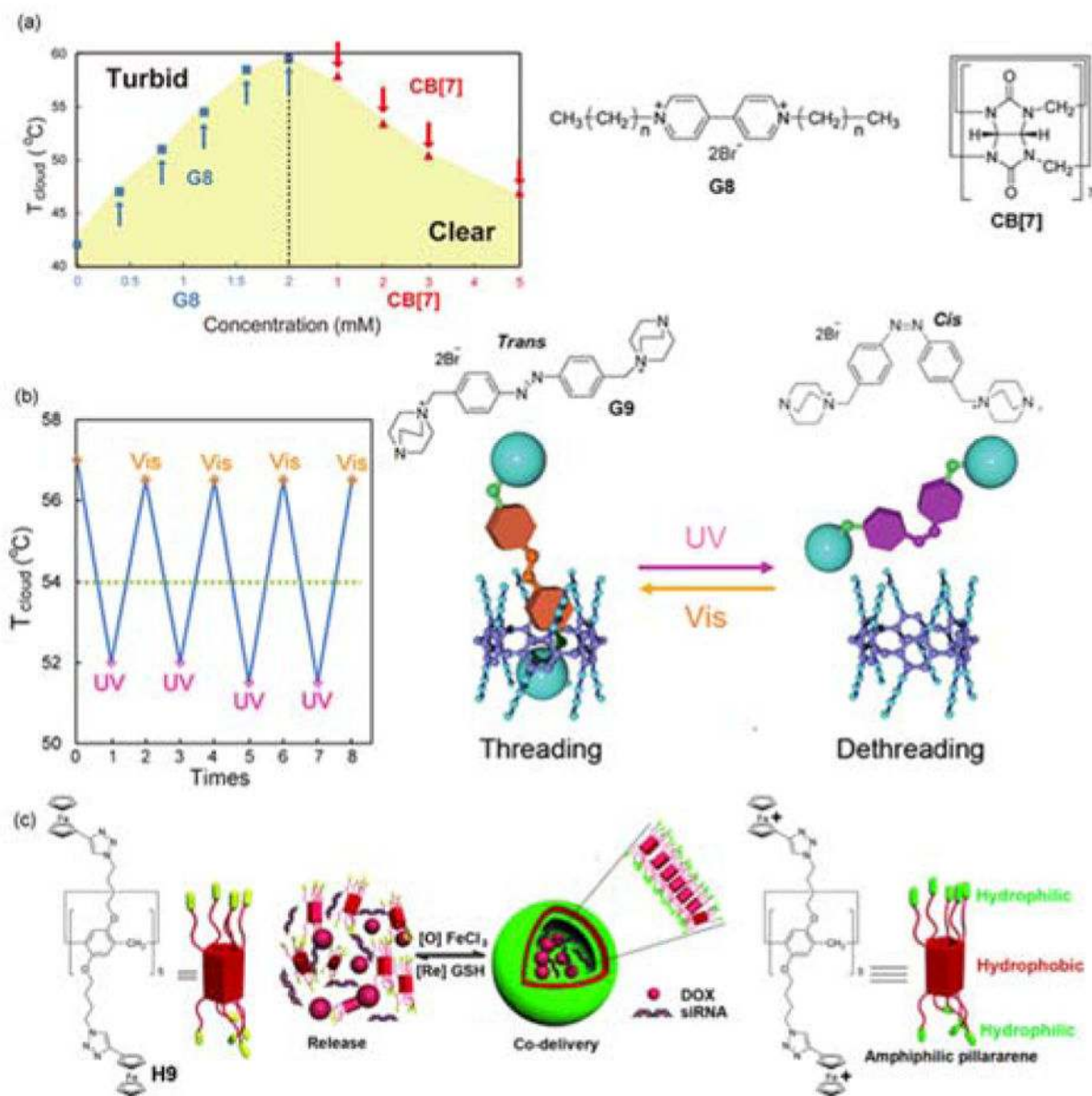
**Fig. 8.** Schematic illustration of the activation of gold nanoparticle (AuNP-NH<sub>2</sub>) cytotoxicity by use of an ultrastable host-guest pair. Reprinted with permission from *Nat. Chem.*, 2010, **2**, 962–966. Copyright 2010, Nature Publishing Group



**Fig. 9.** (a) Synthesis of pillar[n]arenes with functional groups, (b) X-ray crystal structures of pillar[5]arene and (c) calculated electron potential profile (DFT, B3LYP/6-31G(d,p)) of a pillar[5]arene bearing 10 methyl substituents.



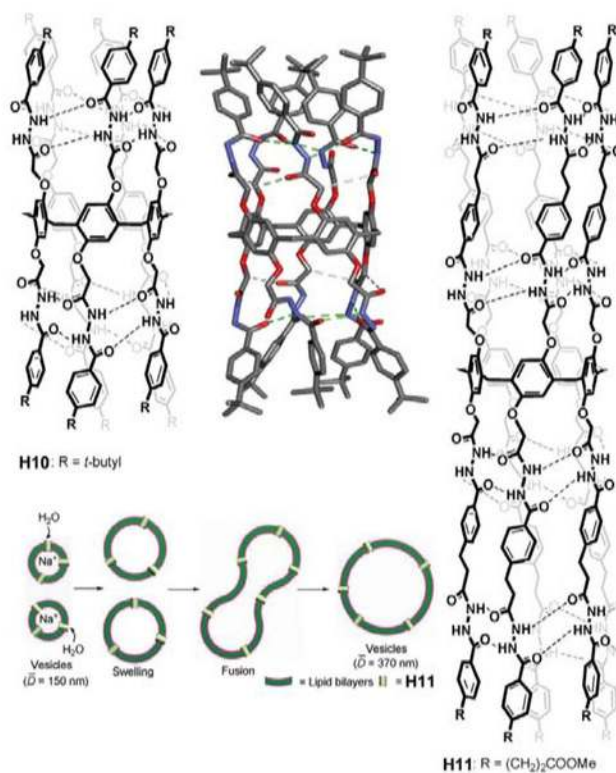
**Fig. 10.** Synthesis of pillar[n]arenes with (a) carboxylate anions, (b) non-ionic tri(ethylene oxide) chains and (c) trimethyl ammonium cations. (d) Guest molecules for pillar[n]arenes in aqueous media.



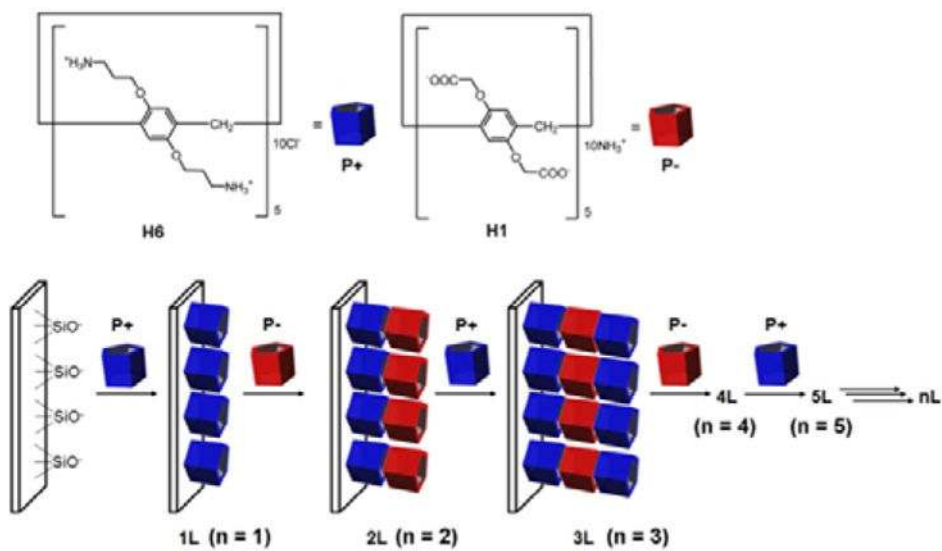
**Fig. 11.**

(a) Chemically responsive lower critical solution temperature (LCST) changes using pillar[5]arene **H7**, viologen guest **G8**, and competitive host **CB[7]**. (b) Photoresponsive LCST changes using pillar[6]arene **H8** and photoresponsive azobenzene guest **G9**. Reproduced with permission from ref 35. Copyright 2012 American Chemical Society. (c) Redox-responsive supramolecular changes between cationic vesicles and precipitates for the release of drug/siRNA materials. Reproduced with permission from ref 36. Copyright 2014 Wiley-VCH Verlag GmbH & Co. KGaA.

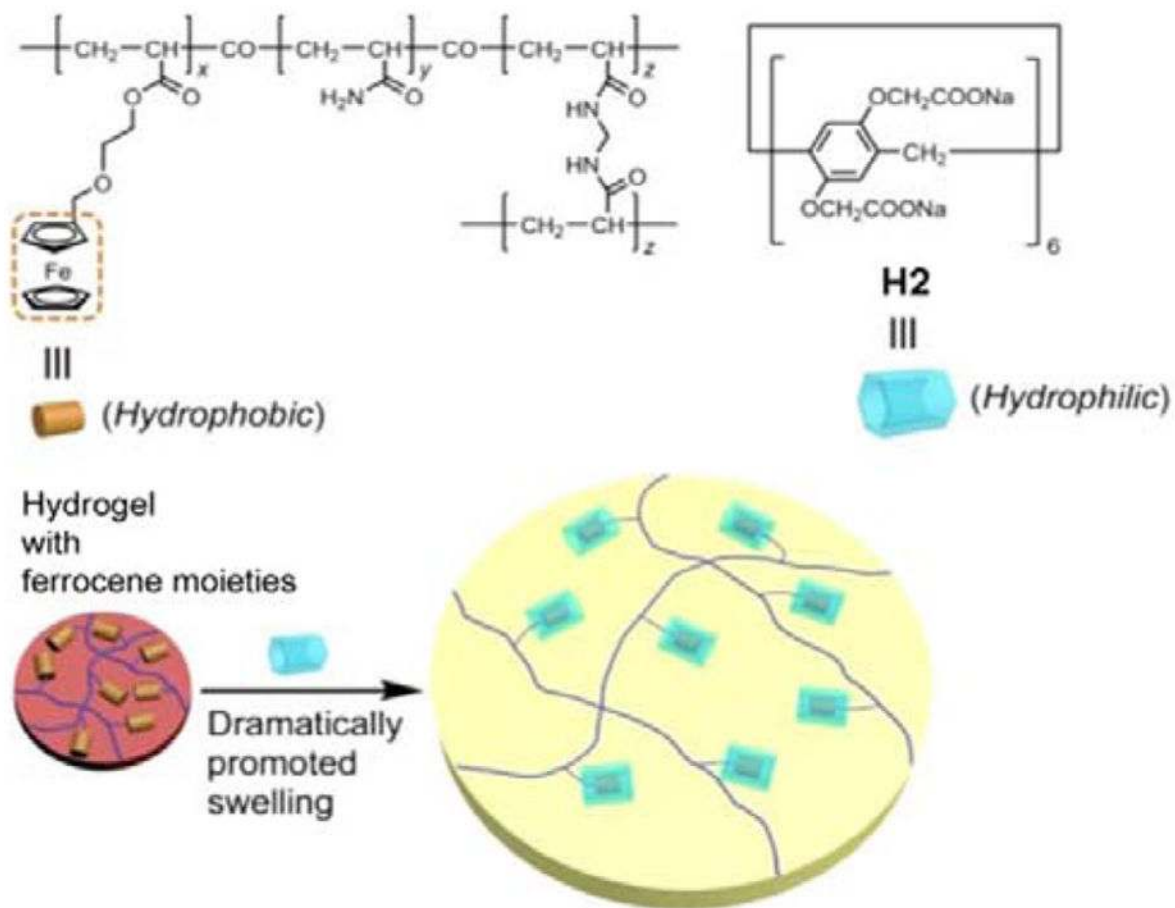


**Fig. 12.**

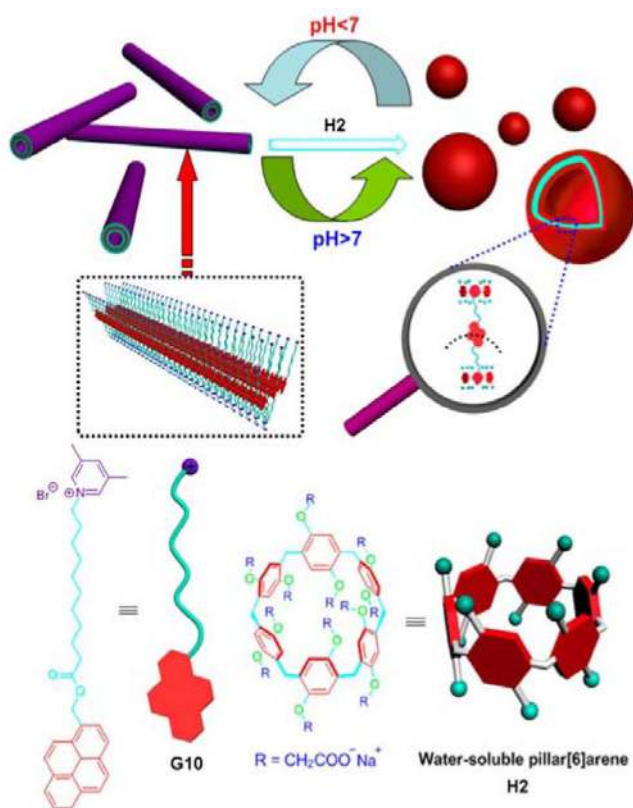
(a) Chemical and X-ray crystal structures of hydrazide-modified pillar[5]arenes (**H10** and **H11**). (b) Schematic representation of the increase in vesicle size caused by **H11**-mediated outside-to-inside water transport. Reproduced with permission from ref 37. Copyright 2012 American Chemical Society.



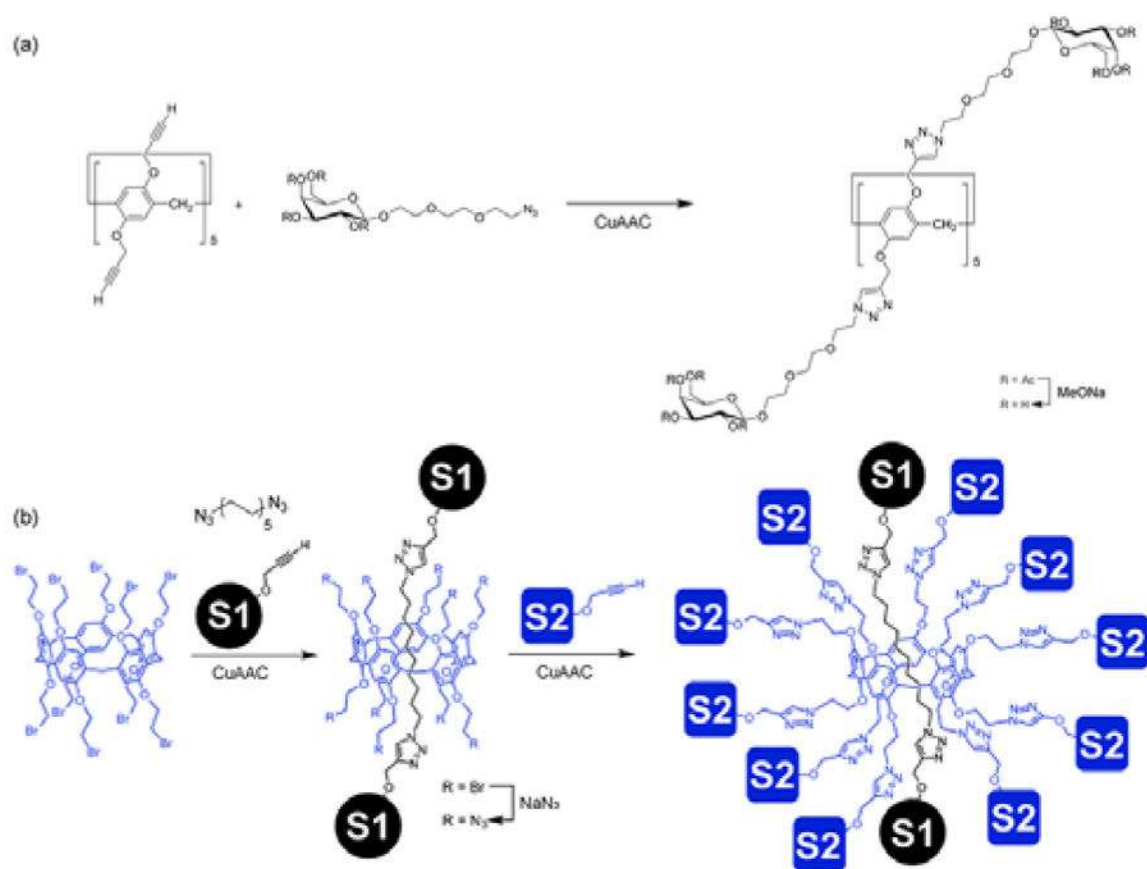
**Fig. 13.** Layer-by-layer assembly through consecutive adsorption of cationic and anionic pillar[5]arenes. Reproduced with permission from ref 38. Copyright 2015 American Chemical Society.



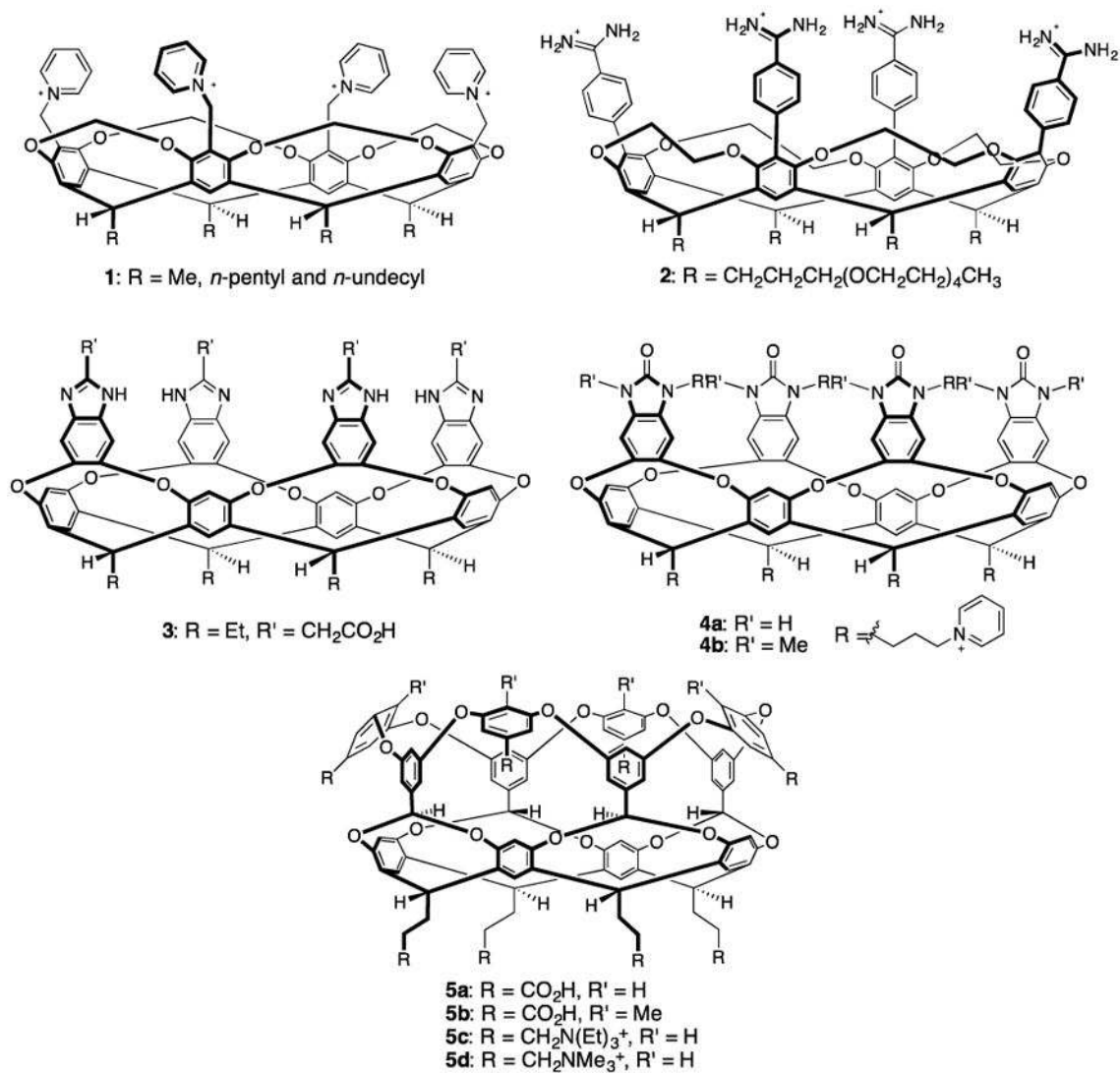
**Fig. 14.** Chemical structures of polymer networks and water-soluble pillar[6]arene **H2**; illustration of the dramatic swelling of the hydrogel promoted by **H2** ferrocene host-guest interactions. Reproduced with permission from ref 39. Copyright 2016 American Chemical Society.



**Fig. 15.** Schematic representations of (top) the reversible *trans*-formations between **G10** nanotubes and **H2G10** vesicles and (bottom) the molecular structures of **H2** and **G10**. Reproduced with permission from ref 40. Copyright 2016 American Chemical Society.

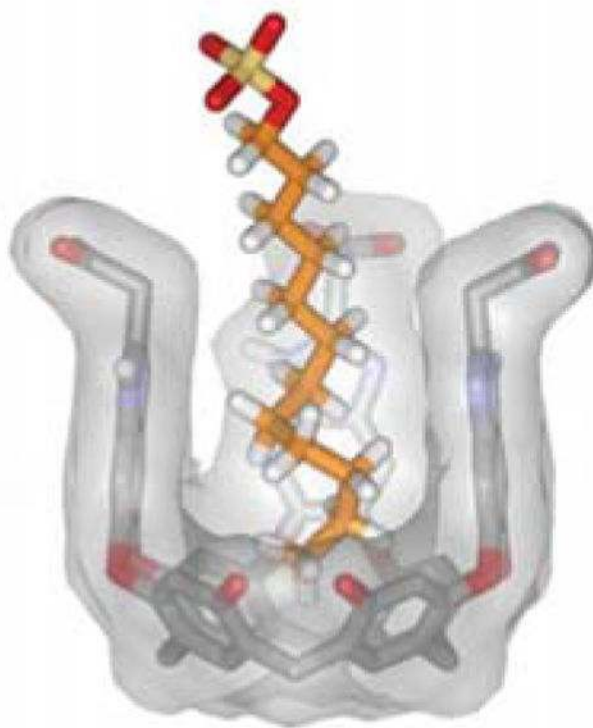
**Fig. 16.**

(a) Synthesis of pillar[5]arene-based glycoclusters from a deca-alkyne pillar[5]arene. (b) Synthesis of [2]rotaxanes containing different sugars on the pillar[5]arene rings and the axle. Reproduced with permission from ref 42. Copyright 2016 Wiley-VCH Verlag GmbH & Co. KGaA.

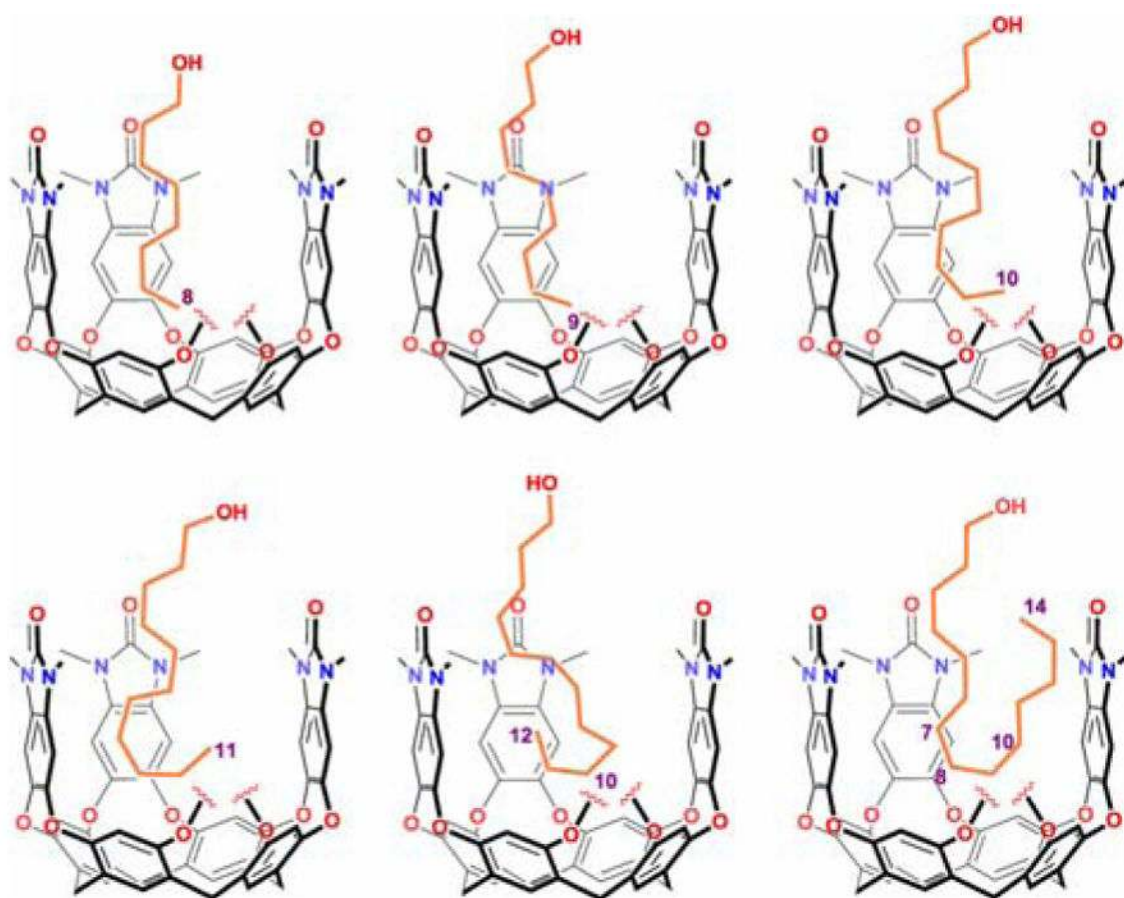


**Fig. 17.**  
Structures of water-soluble deep-cavity cavitands.

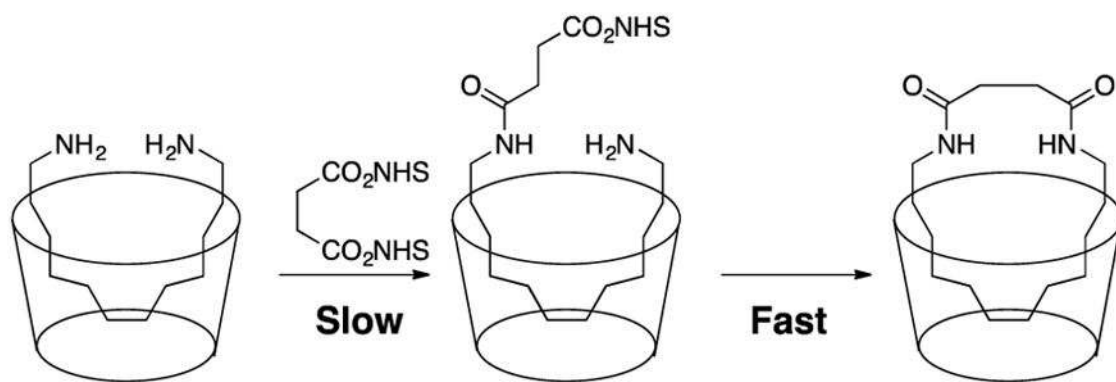




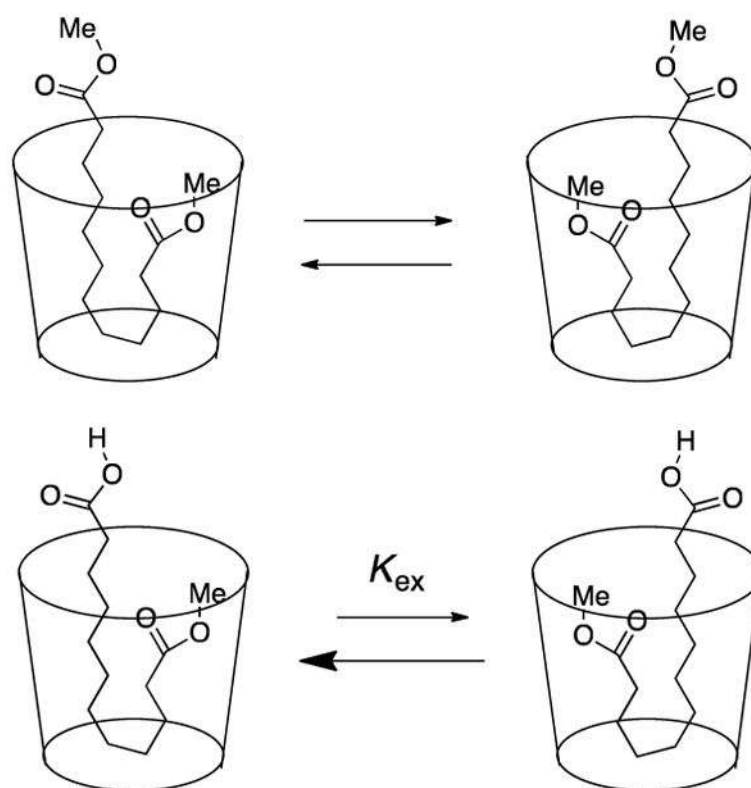
**Fig. 18.** Representation of the sodium dodecylsulfate–cavitand **3** complex in D<sub>2</sub>O showing eight carbons of the chain in a helical conformation. (Adapted from Ref. 43 with permission from The Royal Society of Chemistry.)



**Fig 19.** Cartoons of the complexes of n-alcohols and host **4b**. The relative positions of the C atoms in the cavitands correspond to the NMR spectra and Nucleus Independent Chemical Shift (NICS) calculations. (Reprinted with permission from *J. Am. Chem. Soc.* 2014, 136 (14), 5264–5266. Copyright (2014) American Chemical Society.)



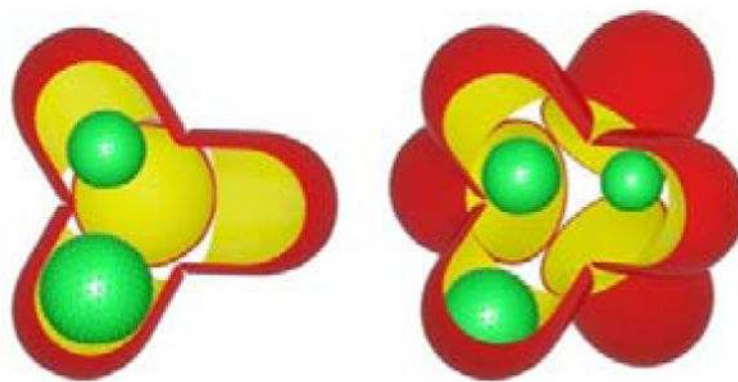
**Fig. 20.**  
Proposed reaction sequence for the cyclization of diamines within **4a**.



**Fig. 21.** Cartoons of folded bola-amphiphiles in cavitand **4b** with (*top*) the diester and (*bottom*) the monoester-monoacid.

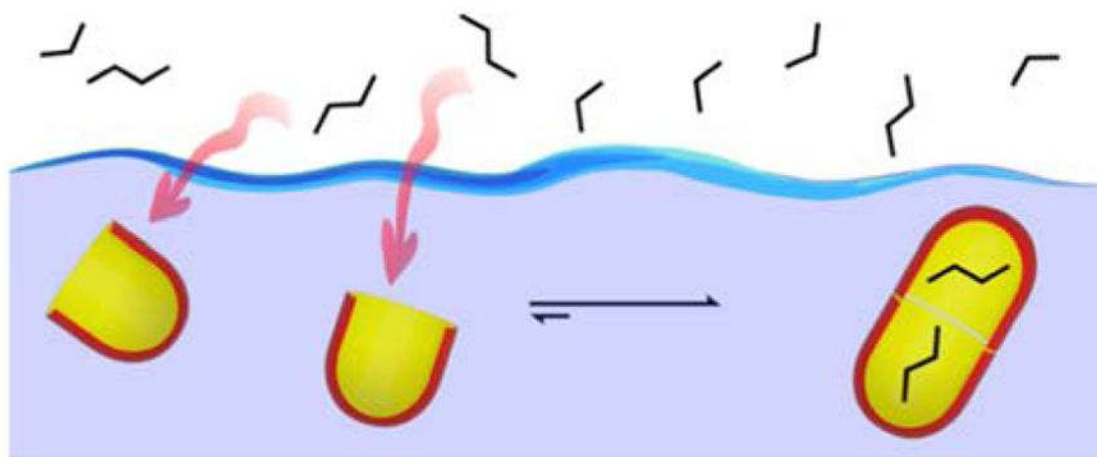


**Fig. 22.**  
Selected packing motifs of alkanes with the dimer of host **5a**.

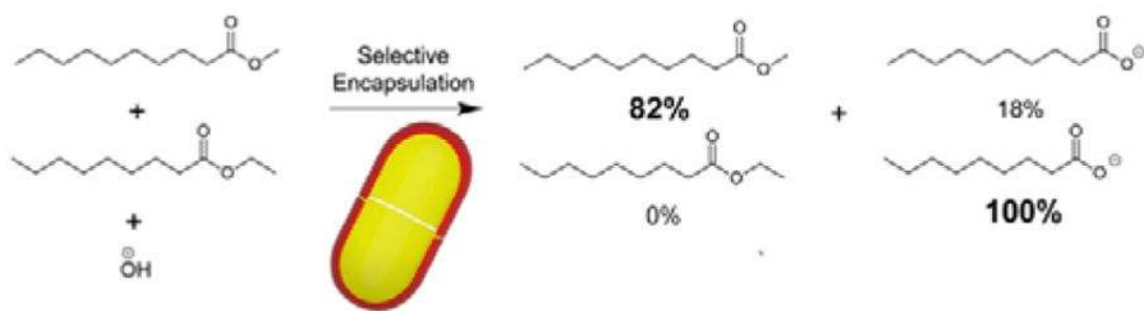


**Fig. 23.** Cartoons of the tetramer (*left*) and hexamer (*right*) assemblies of TEMOA. Select surfaces are cut away to reveal the two and three guests in each respective assembly.



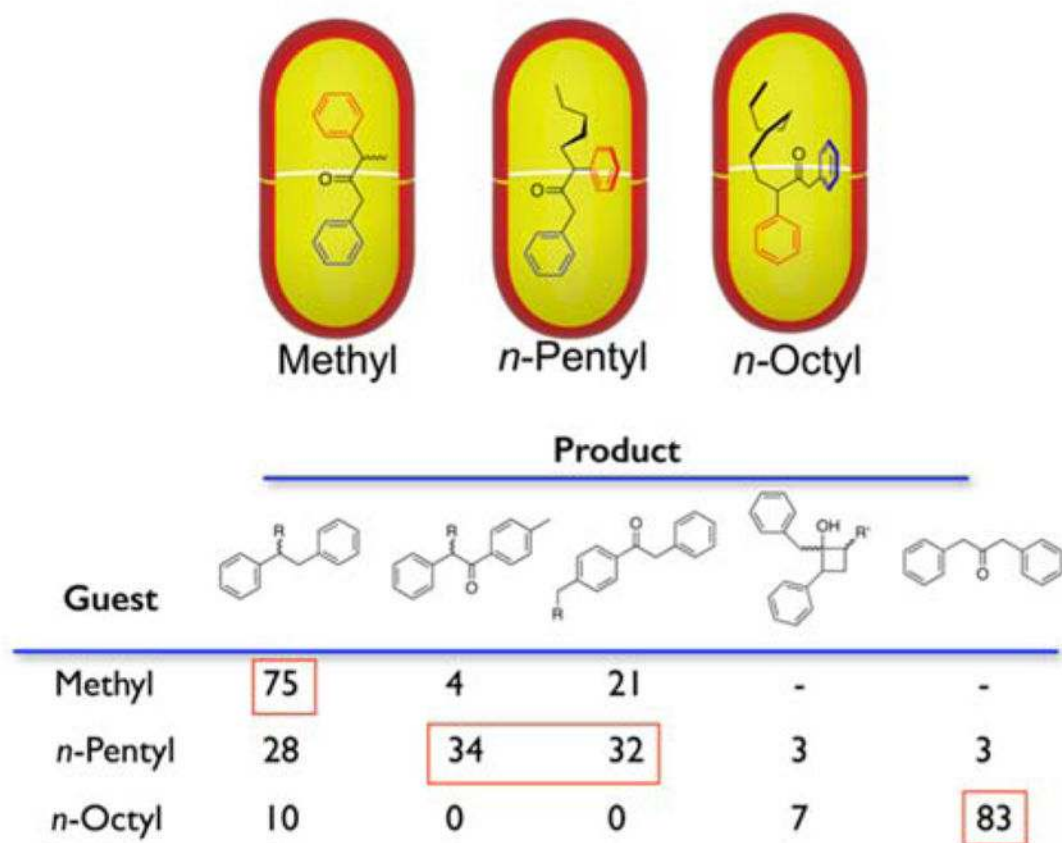


**Fig. 24.**  
Physical separation of hydrocarbon gases using host **5a**.

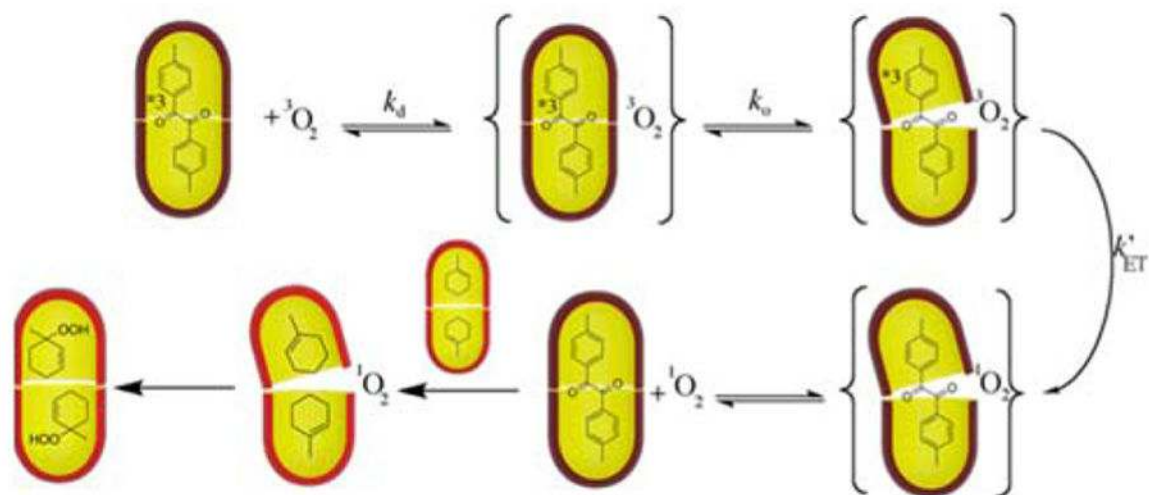


**Fig. 25.**

An example of the kinetic resolution of methyl ester and ethyl ester within dimer **5a2**.



**Fig. 26.** Summary of how the supramolecular capsule 5a<sub>2</sub> templates the packing motifs of α-(*n*-Alkyl) dibenzyl ketones and consequently control their excited-state chemistry.

**Fig. 27.**

Proposed mechanism of the selective oxidation in capsule **5a<sub>2</sub>**: 1) generation of triplet encapsulated DMB; 2) capsule opening to allow contact between oxygen and triplet DMB, and subsequent energy transfer; 3) escape of singlet oxygen from the capsule into bulk solution; and 4) entry of singlet oxygen into the alkene-containing capsule and regioselective oxidation.